

Annual Review of Biophysics

The Contribution of Biophysics and Structural Biology to Current Advances in COVID-19

Francisco J. Barrantes

Biomedical Research Institute (BIOMED), Catholic University of Argentina (UCA)–National Scientific and Technical Research Council, Argentina (CONICET), C1107AFF Buenos Aires, Argentina; email: francisco_barrantes@uca.edu.ar

Annu. Rev. Biophys. 2021. 50:493–523

The *Annual Review of Biophysics* is online at
biophys.annualreviews.org

<https://doi.org/10.1146/annurev-biophys-102620-080956>

Copyright © 2021 by Annual Reviews.
All rights reserved

Keywords

COVID-19, SARS-CoV-2, ACE2, X-ray diffraction, cryo-electron microscopy, virus–receptor interactions

Abstract

Critical to viral infection are the multiple interactions between viral proteins and host-cell counterparts. The first such interaction is the recognition of viral envelope proteins by surface receptors that normally fulfil other physiological roles, a hijacking mechanism perfected over the course of evolution. Severe acute respiratory syndrome coronavirus 2 (SARS-CoV-2), the etiological agent of coronavirus disease 2019 (COVID-19), has successfully adopted this strategy using its spike glycoprotein to dock on the membrane-bound metalloprotease angiotensin-converting enzyme 2 (ACE2). The crystal structures of several SARS-CoV-2 proteins alone or in complex with their receptors or other ligands were recently solved at an unprecedented pace. This accomplishment is partly due to the increasing availability of data on other coronaviruses and ACE2 over the past 18 years. Likewise, other key intervening actors and mechanisms of viral infection were elucidated with the aid of biophysical approaches. An understanding of the various structurally important motifs of the interacting partners provides key mechanistic information for the development of structure-based designer drugs able to inhibit various steps of the infective cycle, including neutralizing antibodies, small organic drugs, and vaccines. This review analyzes current progress and the outlook for future structural studies.

**ANNUAL
REVIEWS CONNECT**

www.annualreviews.org

- Download figures
- Navigate cited references
- Keyword search
- Explore related articles
- Share via email or social media

Contents

1. INTRODUCTION	494
2. OVERALL STRUCTURE OF THE SARS-COV-2 VIRION	495
3. THE MOLECULAR MACHINERY INVOLVED IN VIRUS-RECEPTOR INTERACTIONS	496
3.1. First Step in Viral Infection: CoV Recognition by Cell-Surface Receptors ...	496
3.2. Cell-Surface Binding: The Viral S Glycoprotein	497
3.3. The Host-Cell Membrane-Embedded Proteases and Their Interaction with the S Protein	497
3.4. Exact Stoichiometry of Virus S1 Protein Receptor Is Still Uncertain	501
3.5. The Receptor Binding Domain of the S Glycoprotein S1 Subunit	502
4. MEMBRANE FUSION: THE S2 FUSOGENIC SUBUNIT AND THE HOST-CELL PROTEASES THAT ENABLE ITS ENGAGEMENT	505
5. WHAT DO THE ENDOGENOUS VIRAL PROTEASES DO?	506
6. STRUCTURAL KNOWLEDGE OPENS NEW AVENUES FOR DRUG, VACCINE, AND ANTIBODY DEVELOPMENTS	507
7. ION CHANNELS IN SARS-COV-2	510
8. STRUCTURE-FUNCTION CORRELATIONS	511
9. OUTLOOK AND PROSPECTS	513
10. CONCLUDING REMARKS	514

COVID-19:

coronavirus disease
2019

SARS: severe acute
respiratory syndrome

CoV: coronavirus

SARS-CoV-2: severe
acute respiratory
syndrome coronavirus
2

HCoV:
human coronavirus

SARS-CoV: severe
acute respiratory
syndrome coronavirus

MERS: Middle East
respiratory syndrome

MERS-CoV: Middle
East respiratory
syndrome coronavirus

1. INTRODUCTION

The ongoing pandemic of coronavirus disease 2019 (COVID-19) caused by the severe acute respiratory syndrome (SARS) coronavirus (CoV) 2 (SARS-CoV-2) constitutes a very serious public health problem worldwide. Some CoVs are enzootic, i.e., restricted to animals, whereas others have crossed the species barrier to become zoonotic diseases in humans. Thus, CoVs cause respiratory, neurological, enteric, and hepatic diseases of varying degrees of severity in animals ranging from birds to Beluga whales. CoVs belong to the subfamily *Coronavirinae* in the *Coronaviridae* family and can be subdivided into four genera: α , β , γ , and δ (28, 65). CoVs pack inside their envelope between 26 and 32 kilobases of single-stranded positive-sense RNA. In general, CoVs have a high frequency of recombination and high mutation rates, which may have allowed them to adapt to a wide variety of ecological niches and hosts (61). The mechanism of cross-species spillover remains poorly understood.

Seven human CoVs (HCoVs) have been identified to date. HCoV-OC43, HCoV-293, HCoV-NL63, and HKU1-CoV generally cause mild, self-limiting respiratory diseases, mainly forms of the common cold; other forms of the common cold are caused by rhinoviruses and the parainfluenza virus, among others. A second category of HCoVs are SARS-CoV and Middle East respiratory syndrome (MERS)-CoV, the etiological agents of SARS and MERS, the causative agents of the epidemics in 2003 and 2012, respectively, which, like the recently emerged SARS-CoV-2 (the agent of COVID-19), are highly pathogenic viruses. The full genome of SARS-CoV-2 shares 79.5% sequence identity with SARS-CoV and 50% with MERS-CoV and is 96% identical to the genomic sequence of the Chinese bat CoV, BatCoV RaTG13 (171).

The reader is referred to comprehensive reviews on the biological and evolutionary aspects (73), epidemiology (122), clinical aspects (31, 106), physicochemical properties (109), and structural biology (34, 133) of CoVs that complement this review.

Cell tropism and the host range of CoVs are largely determined by structural modifications occurring in the spike (S) proteins during evolution, involving variations in their amino acid residue exposure, stability, and resulting dynamics. Only a few weeks after the outbreak of COVID-19 and the discovery of SARS-CoV-2, there was an explosion of high-resolution X-ray crystallographic and cryo-electron microscopy (cryo-EM) studies on the structure of the viral S proteins alone or in complex with the virus cell-surface receptor, the metalloprotease angiotensin-converting enzyme 2 (ACE2), and of other proteases key to the viral cell cycle. This would have been an impossible task to achieve in such a short time were it not for the pioneering crystallography work begun almost two decades ago on the structure of the related SARS-CoV and MERS-CoV (69, 124). This is a brilliant example of how the field of biophysics has been positioned at the forefront of research to contribute swiftly in a crisis of global proportions.

cryo-EM:

cryo-electron microscopy

nsp: nonstructural protein

RdRp:

RNA-dependent RNA polymerase

2. OVERALL STRUCTURE OF THE SARS-COV-2 VIRION

The cryo-EM images of the SARS-CoV-2 virion isolated from the supernatant of infected VeroE6 cells show roughly spherical bodies with a diameter of 91 ± 11 nm (50), i.e., very similar to other members of the *Coronaviridae* (92, 93, 152). The early transmission EM images obtained by June Dalziel Almeida of “previously uncharacterized human respiratory viruses” in the late 1960s were the first observations of the spikes at the surface of the virion that gave rise to the hitherto unknown genus of CoVs (1). CoVs possess four main structural proteins, which are assembled at the endoplasmic reticulum–Golgi intermediate compartment (ERGIC) of the host cell (59): nucleocapsid (N), S, envelope (E), and membrane (M) proteins (**Figure 1**). In addition, their genome codes for 16 nonstructural proteins (nsp1–nsp16) involved in key aspects of the CoV replication cycle, such as papain-like protease (PL^{PRO}), 3-chymotrypsin-like protease (3CL^{PRO}) or main protease (M^{PRO}), RNA-dependent RNA polymerase (RdRp), helicase, and exonuclease. PL^{PRO} is a domain of nsp3. Eight accessory proteins named by their open reading frame (orf) succession (orf3a, orf6, orf7a, orf7b, orf8, orf9b, orf9c, and orf10) are present in this type of virus (21).

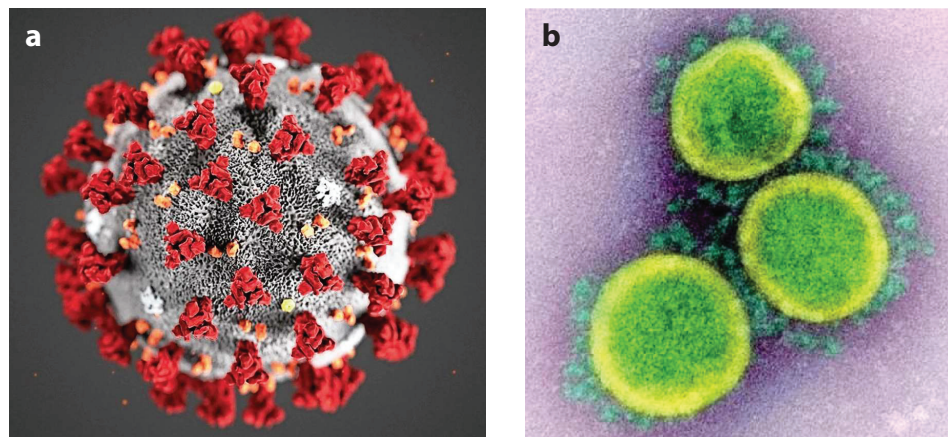


Figure 1

(a) Schematic diagram of severe acute respiratory syndrome coronavirus 2 (SARS-CoV-2) showing the membrane protein, the envelope protein, and the spike protein. Model created by Alissa Eckert and Dan Higgins at the Centers for Disease Control and Prevention. (b) Pseudocolored negatively stained electron micrograph of SARS-CoV-2. The spikes of the virus are clearly visible surrounding the perimeter of the envelope sphere. Both images are public domain illustrations obtained through the Public Health Image Library and the National Institute of Allergy and Infectious Diseases of the National Institutes of Health.

The N protein is a homodimer that resides together with the genomic RNA in the ribonucleoprotein (RNP) core inside the envelope. Early EM observations showed that the RNP complex released from HCoV-229E is a helix 14–16 nm in diameter and up to 320 nm in length (78). The RNP–genome complex is packed inside a capsid of variable size, from an 84 nm mean diameter for murine CoV (M-CoV, MHV) (94) to 120 nm in the case of the bottlenose dolphin BCoV HKU22 virus, a γ -CoV, the largest observed to date for RNA viruses (66, 122, 150). The N protein chaperones and provides protection to the RNA genome, particularly during its replication cycle and transit along the ERGIC during the viral cycle in the host cell.

The M protein is a major component of the viral envelope. It is an integral membrane glycoprotein whose main functions are to adapt a region of the membrane for virus assembly and help define the shape of the viral envelope. It can adopt two conformations, elongated and compact. Elongated M proteins rigidize the membrane and produce the aggregation of S proteins in clusters; compact M proteins are associated with a more flexible membrane with low spike density (94). In the case of SARS-CoV, once the virion is internalized, the interaction of the M protein with the S protein is required for retention of S protein in the ERGIC (89).

The E protein is a substoichiometric (relative to the other structural proteins) component of CoVs whose precise function is still unknown except that it has ion channel properties, for which reason it is classified as a viroporin (131). It is currently assumed that the E protein contributes to the later stages of the virion cycle in the infected cell—the assembly and the budding processes (94). It is a small (76- to 109-amino-acid) integral membrane protein with a short hydrophilic amino-terminus, a relatively long hydrophobic transmembrane domain, and a long carboxy-terminus (160). Mutagenesis of its helical hydrophobic transmembrane domain alters virus replication, which is restored upon reestablishing the native α -helical structure. Restored E protein is more sensitive to treatment with the ion channel inhibitor hexamethylene amiloride (160). The E protein of MHV CoV-A59 localizes at the ERGIC membranes and subsequently at the Golgi complex, but its role in virion morphogenesis is not known. The E protein does not traffic to the cell surface (136). It should be mentioned that the E protein is not the only ion channel molecule in CoVs, as discussed in Section 7 of this review.

The S protein structure is analyzed in detail in the sections below.

3. THE MOLECULAR MACHINERY INVOLVED IN VIRUS–RECEPTOR INTERACTIONS

3.1. First Step in Viral Infection: CoV Recognition by Cell-Surface Receptors

The appearance of ligand recognition in living organisms has occurred in various instances as a consequence of coevolution between interacting partners. However, the crosstalk between the CoV infective molecular machinery and eukaryotic cell-surface receptors may differ from this co-evolutionary mechanism because the receptors, which are transmembrane proteases in the case of CoVs, fulfill preexisting physiological roles in eukaryotic cells (e.g., blood pressure regulation via cleavage of angiotensin II in the case of ACE2), which these viruses exploit to serve their own specific purpose through plastic adaptations. One reason why ACE2 is selected by the virus as a target molecule is probably the ubiquitous distribution of the membrane-bound enzyme in many tissues, particularly mucosal epithelia. The architecture of the mucosae lining, for instance, the intestinal tract is designed to maximize surface expanse for nutrient absorption, offering the virus abundant surface area for its landing on the apical membrane surface. Subsequently, the virions could diffuse by randomly walking the membrane until they collide with their target receptors, in a typical reduction of dimensionality process that enhances successful encounters with receptors. It has been

hypothesized that ancestral forms of CoVs may have lacked parts of the host-cell receptor recognition machinery and thus relied on this two-dimensional diffusion mechanism to reach their targets (see below). Epithelial cells lining the oral (33, 156), nasal (33, 98, 176), bronchoalveolar (54, 147, 171), and enteric (36, 46, 62) mucosae cover an enormous area in mammalian organisms; this combined area is dominated by the upper respiratory tract and pulmonary alveolar area, with values of $118 \pm 22 \text{ m}^2$ and $91 \pm 18 \text{ m}^2$ in male and female humans, respectively (16), and the enteric mucosa, with an even larger total surface of 260–300 m^2 (35). In vitro, polarized epithelial cell cultures show predominant ACE2 expression at the apical cell surface rather than at the basolateral membranes; SARS-CoV uses the apical plasmalemma to infect epithelium (43). Similarly, SARS-CoV-2 utilizes this target surface in human mucosae (171). Thus, the initial molecular recognition and binding steps are intimately linked to viral cellular tropism.

3.2. Cell-Surface Binding: The Viral S Glycoprotein

By the time of the first CoV epidemic, our understanding of the biology, biochemistry, and molecular biology of CoVs was quite advanced; it is therefore not surprising that the pioneer X-ray crystallographic studies of CoV addressed the surface S glycoprotein, the region of the virus that plays the central role in binding to its receptor and infection at large. The S protein is a trimer composed of three S1–S2 subunit heterodimers. With negative staining EM (68) (see **Figure 1b**) or, more recently, cryo-EM (50, 163, 165), the S protein trimer ectodomain of CoVs appears as a clover-shaped body approximately $25 \pm 9 \text{ nm}$ long, with a stalk formed by a trimer of S2 subunits and three heads of S1 subunits. In cryo-EM, the predominant form observed at the surface of intact virions is the clover-shaped body, which corresponds to the prefusion conformers; a less abundant, extended, thin morphology, attributable to the postfusion conformer, is also observed (50). Coverage of the SARS-CoV-2 surface by S protein trimers is sparse: The density is approximately 1 spike/500 nm^2 (50).

Each S1 N-terminal region contains a receptor binding domain (RBD), the region recognized by the counterpart surface of the ACE2 receptor. **Figure 2a** shows the prefusion structure of the S1 protein, highlighting the two conformations of the RBD, down (closed) and up (open), the latter corresponding to the binding-enabled conformer in only one of the S1 protomers. The trimeric morphology is more readily apparent in end-on views, exemplified in **Figure 2b,c**, which shows the cryo-EM electron density of the MERS-CoV.

Each trimer of the S glycoprotein of SARS-CoV-2 contains 66 N-linked glycosylation sites in its glycan moiety, apparently involved in viral protein folding, stability, and tropism (145) and shielding of the virus from the host defense mechanisms (7). The glycosylation sites are under selective pressure and camouflage viral epitopes from being recognized and neutralized by host antibodies. This immune evasion mechanism is also observed with the human immunodeficiency virus (HIV) envelope glycoprotein (116).

3.3. The Host-Cell Membrane-Embedded Proteases and Their Interaction with the S Protein

Over the course of its evolution, ACE2 has acquired the capacity to interact with quite a few host-cell proteases that aid in the viral infection process, such as cathepsins L and B, trypsin, elastase, furin, TMPRSS2, and TMPRSS4 (88). In addition to ACE2, the surface glycoprotein CD147, also termed Basigin or EMMPRIN, has been purported to act as a receptor for SARS-CoV-2 (141). CD147 is a member of the immunoglobulin superfamily. Interestingly, an antagonist of CD147, peptide-9, inhibits the binding of SARS-CoV-2 to HEK293 cells (141).

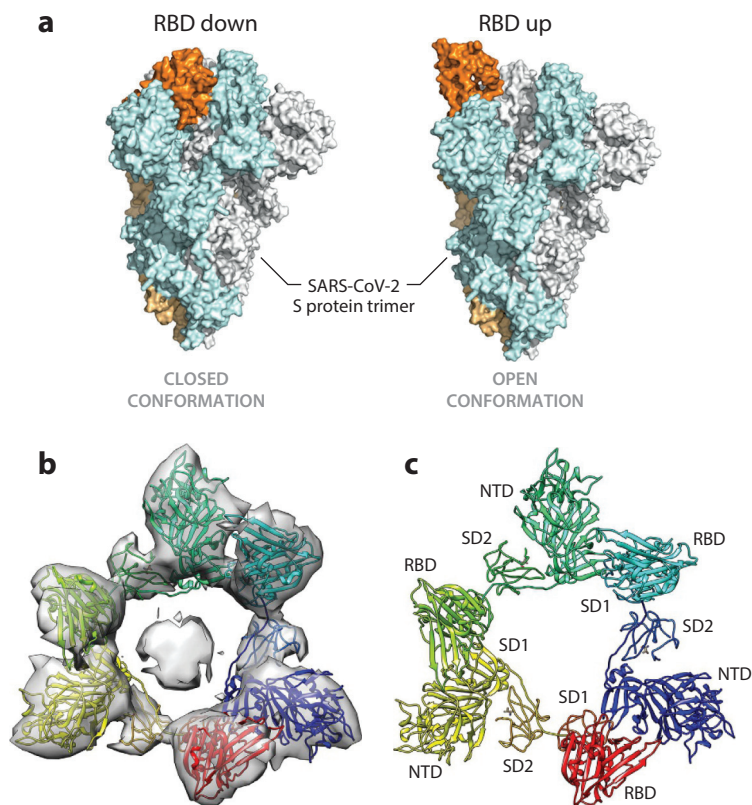


Figure 2

(a) Lateral view of the S glycoprotein trimer of SARS-CoV-2 in the closed (*left*, PDB ID 6vxx) and open (*right*, PDB ID 6vyb) crystal forms. The three protomers are colored light cyan, gray, and light orange. Buried in the closed state, the RBD (*orange*) from one of the protomers (*light orange*) swings up in the open, binding-ready conformation (169). (b) Low-resolution cryo-EM electron density of the overall structure of the dissociated S1 trimer of MERS-CoV. (c) Ribbon rendering of the MERS-CoV S1 trimer, including the three NTDs, RBDs, SD1s, and SD2s of each protomer in the trimer (165). Figure reproduced from open access articles distributed under the terms of the Creative Commons CC BY license. Abbreviations: EM, electron microscopy; MERS-CoV, Middle East respiratory syndrome coronavirus; NTD, N-terminal domain; PDB, Protein Data Bank; RBD, receptor binding domain; S, spike; SARS-CoV-2, severe acute respiratory syndrome coronavirus 2; SD, subdomain.

The recent X-ray and cryo-EM structures of the SARS-CoV-2 S protein, as well as recently discovered details of the RBD that resides in the S1 subunit and of its membrane-bound cognate receptor, the enzyme ACE2 in complex with the S1 subunit, have delivered invaluable information on the mechanism of SARS-CoV-2 recognition and binding to the host-cell surface (63, 110, 137, 152, 159). As stated in Section 1, this tour de force could be accomplished in an unprecedentedly short time partly because of the groundwork that preceded it and the new capabilities of cryo-EM techniques. In this section, we analyze the new data and draw comparisons with the known structures and mechanisms of related viruses.

Historically, of the two binding partners, ACE2's structure was the first to be solved at the atomic scale. ACE2 is the enzyme that catalyzes the hydrolysis of angiotensin II into angiotensin (1–7). It is an 805-amino-acid long transmembrane glycoprotein with metallopeptidase enzymic

activity. In contrast to its closest homolog, the somatic ACE peptidyl dipeptidase enzyme ACE, ACE2 displays carboxypeptidase activity. The catalytic domains of the two enzymes are 42% identical (134). ACE2 purified from Vero E6 cells was found to be the receptor for SARS-CoV, and a soluble form of the enzyme was shown to inhibit the binding of the S1 subunit of the virus to ACE2-expressing cells (72). ACE2 is a glycoprotein, and its glycans at two glycosylated sites, N90 and N322, contribute in an opposite manner to the virus–ACE2 binding interaction, as demonstrated by a recent *in silico* molecular dynamics study (86). N90 partly covers the binding interface, interfering with the docking of S1 onto ACE2, whereas N322 interacts tightly with the RBD of S1 in its bound state, binding to a conserved region previously identified as a cryptic epitope for a neutralizing antibody (172).

The similar architectural design of the CoV spike proteins is indicative of the similar mechanistic strategies developed to infect cells. CoVs have chosen membrane-bound proteases to accomplish this task. Thus, human H229E-CoV, transmissible gastroenteritis virus, porcine epidemic diarrhea virus, and feline infectious peritonitis virus are recognized by another zinc metalloprotease, aminopeptidase N [APN, also known as cluster of differentiation 13 (CD13)] (70). MHV, a β -CoV, employs mouse cell adhesion carcinoembryonic antigen-related cell adhesion molecule 1 (mCEACAM1) to bind its S1 N-term domain (60). The host-cell receptor molecule hijacked by MERS-CoV is the enzyme dipeptidyl-peptidase 4 (DPP4), also known as CD26 (65, 71).

Studies of ACE2 were preceded by X-ray determination of the structure of the human testicular ACE in complex with the inhibitor lisinopril [N2 -[(S)-1-carboxy-3-phenylpropyl]-L-lysyl-L-proline] at 2.0 Å resolution (91). On the basis of this structure, a homology model was produced suggesting the complementarity of the viral binding domain of ACE2 and the SARS-CoV S1 protein (102). One year later, Carfi and collaborators (124) studied the X-ray structure of the proteolytically stable core of SARS-CoV. The crystallographic data of this β -CoV constituted one of the first descriptions at the atomic level. This was followed in 2005 by a key X-ray diffraction study at 2.9 Å of the SARS-CoV S glycoprotein in complex with human ACE2 by Harrison and coworkers (69). The combined crystallographic data disclosed two domains in ACE2: the core region (124) and the RBD, comprised of the residues between 306 and 527, within which a loop formed by residues 424–494 corresponded to the receptor binding motif (RBM) in SARS-CoV.

In addition to the three proteases acting as receptors for CoVs, the evolutionarily versatile MERS-CoV was also found to infect host cells upon binding to a completely different type of host-cell receptor, i.e., the oligosaccharide moieties of surface glycoproteins; the binding to α 2,3-sialoside sites is highly specific but of low affinity (71). Cryo-EM disclosed the structure of the MERS S protein region involved in interactions with the receptor carbohydrates: It is a conserved groove (**Figure 3**), different from the RBD, located at the peripheral region of the S1 subunit trimer (97).

HCoV-NL63, a respiratory virus, is the only human α -CoV that uses ACE2 as its receptor (SARS-CoV and SARS-CoV-2 belong to the β). Wu and coworkers (153) determined the structure of the RBD of the HCoV-NL63 complexed with human ACE2 using cryo-EM. The HCoV-NL63 RBD showed two layers of β -sheets (a beta-sandwich) and three discontinuous RBMs that contact ACE2. HCoV-NL63 and SARS-CoV have no structural homology in RBD cores or RBMs, yet the two viruses recognize common ACE2 regions, leading Wu and coworkers to postulate the occurrence of a “virus-binding hotspot” on ACE2 (153, p. 19970). Interestingly, among α - (also called group 1) CoVs, RBD cores are conserved, but RBMs are variable, providing a plausible explanation for how these viruses can recognize different receptors (153). Along these lines, a recent phylogenetic study postulates that SARS-CoV-2 could potentially recognize ACE2 isoforms from various animal species (139).

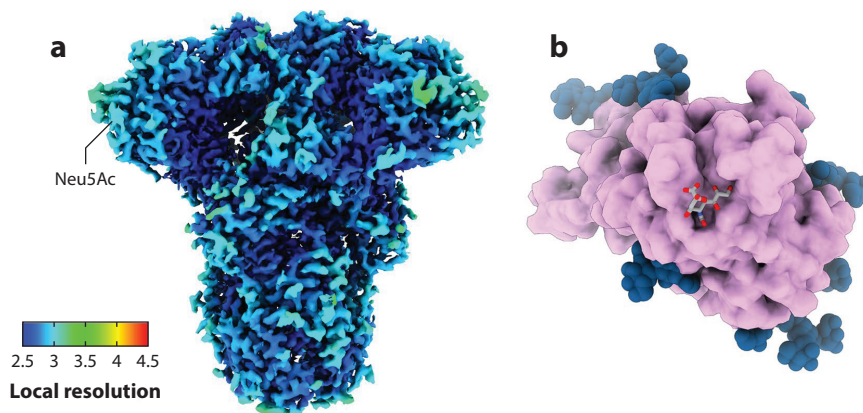


Figure 3

Surface rendering representation of the MERS-CoV S glycoprotein showing the location of the crevice where interaction with its receptor's neuraminic acid (Neu5Ac) occurs. (a) Local resolution map, calculated using cryoSPARC, as indicated in the color-coded scale. (b) Detail of the region (lilac) surrounding the crevice. The receptor's neuraminic acid molecule is shown in gray-red stick rendering. Figure adapted from Reference 97, which is made available via the PMC Open Access Subset for unrestricted research re-use and secondary analysis in any form or by any means with acknowledgement of the original source for the duration of the World Health Organization declaration of COVID-19 as a global pandemic. Abbreviations: COVID-19, coronavirus disease 2019; MERS-CoV, Middle East respiratory syndrome coronavirus; S, spike protein.

Another human β -CoV, HKU1-CoV, in contrast to the related pathogenic β -CoVs SARS-CoV and MERS-CoV, causes mild, predominantly respiratory disease. Its structure in the prefusion conformation was solved at 4.0 Å resolution using single-particle cryo-EM (55). At that time, the receptor for HKU1-CoV was not known, but antibodies against the C-terminal domain (CTD) blocked infection, suggesting that this region of the virus was responsible for attaching to the target cell. The cryo-EM structural data of the S1 protein–ACE2 complex revealed that only one S1 RBD of the trimeric S glycoprotein binds ACE2, adopting an open, protruding up conformation much like that of other CoVs (see **Figure 2**), which enables it to recognize the ACE2 site while keeping the fusion S2 domain distant from this target. The prefusion conformer of the porcine epidemic diarrhea (PEDV) α -CoV S protein, solved using cryo-EM at 3.1 Å, has provided more information on the heterogeneity of conformational states that the S protein undergoes to make the RBD accessible for host-cell binding to its receptor, APN (151).

The structure of the SARS-CoV-2 S protein homotrimer was initially solved in its prefusion stage by Wrapp et al. (152) and Walls et al. (137) using cryo-EM. The former study found that the structure of the SARS-CoV-2 S protein is quite similar to that of the human β -CoV HKU1-CoV, obtained using cryo-EM (55). The cryo-EM study by Walls et al. identified the occurrence of two conformers of the SARS-CoV-2 S protein—open and closed—as has been observed in other CoVs. The closed conformer corresponds to the prefusion structure proper, since the three RBDs of the S protein homotrimer lie flat in a down position, buried at the interface between the three protomers, whereas the open conformer, which is the predominant form, shows one RBD protruding in an up state, ready for binding to ACE2.

Furin is a membrane-bound enzyme of the subtilisin-like proprotein convertase family that cleaves sections of recently synthesized inactive proteins to render them active. Detaching some redundant amino acid motifs (four Pro-Arg-Arg-Ala sequences) in the SARS-CoV-2 S protein enables the activation of S1 to its binding-ready conformer (110, 137). Wrapp et al. (152)

described the presence of a furin proteolytic site at the S1–S2 boundary—a feature absent in other CoVs like SARS-CoV and apparently unique to SARS-CoV-2 in the CoV clade, as is shown by sequence analyses (18). Furin cleavage overcomes the apparently default state (mostly in the down conformation) of the SARS-CoV-2 spike RBD, which is inefficient for host-cell binding. Another cryo-EM study of the SARS-CoV-2 S protein confirmed the furin cleavage site between the S1 and S2 subunits (146). The cryo-EM studies also revealed the solvent accessibility of the S1/S2 region rendered available by the furin cleavage interactions with cell-surface receptors (146, 152). Other studies indicate the coexistence of pre- and postfusion homotrimeric conformers on the surface of mature SARS-CoV-2 virions (7) with a statistically predominant prefusion form, which occurs in three varieties: fully closed (approximately 41%) trimers, trimers with one RBD up (45%), and trimers with two RBDs in the open up conformation (13%) (50).

3.4. Exact Stoichiometry of Virus S1 Protein Receptor Is Still Uncertain

The ratio between virus spikes and host-cell membrane-bound receptor sites varies among CoVs because of the nature of the cell-surface receptors. For example, one of the MERS-CoV S1 domains of its spike protein trimer binds a homodimeric CD26 (DPP4) molecule, its host-cell membrane-bound receptor, enabling the two other S1 domains of the trimer to bind two additional CD26 receptors and giving rise to a complex supramolecular structure consisting of arrays of receptors recruited by S proteins (**Figure 4a**). In contrast, the consensus view is that the SARS-CoV-2 RBD binds one extracellular peptidase domain of ACE2 in a one-to-one molar ratio (38, 69, 118, 146) (**Figure 4b**). However, one ACE2 receptor can apparently recruit two S trimers of SARS-CoV-2 (159). In solution, a spike protein can bind up to three ACE2 ectodomains in a pH-dependent manner (172), suggesting a potential binding capacity like that of MERS-CoV. This study also indicates that the S1 domain evades potentially neutralizing antibodies by conformationally masking a cryptic epitope that can be disrupted by pH changes.

A cryo-EM study of the S1 protein trimer–ACE2 complex of SARS-CoV (118) described a peculiar supramolecular structure of the postfusion conformation: The complexes were found to

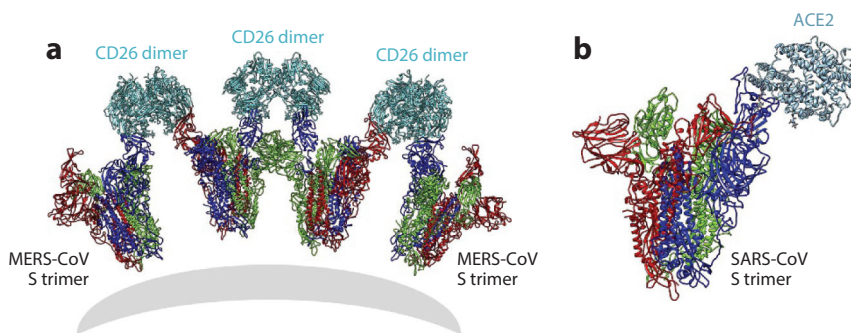


Figure 4

Models of MERS-CoV and SARS-CoV S trimers bound to their receptors. The models were built by superimposition of the S trimer structures with the RBD–receptor complex structures through the RBD domains. (a) The MERS-CoV S trimer can crosslink the homodimeric CD26 receptor during binding, enabling the binding of the two additional S1 subdomains of the trimer, whereas (b) the SARS-CoV S trimer can bind one monomeric ACE2 receptor in a 1:1 complex. Figure adapted from Reference 165, held under Creative Commons license. Abbreviations: ACE2, angiotensin-converting enzyme 2; CD26, cluster of differentiation 26; MERS-CoV, Middle East respiratory syndrome coronavirus; RBD, receptor binding domain; S, spike; SARS-CoV, severe acute respiratory syndrome coronavirus.

cluster together and adopt a rosette-like structure (118). The authors of this study hypothesized that the opening of the SARS-CoV S1 subunit upon binding to the ACE2 receptor may promote the release of the S1–ACE2 complex and S1 monomers from the prefusion spike, triggering the conformational transition from prefusion to postfusion conformers.

3.5. The Receptor Binding Domain of the S Glycoprotein S1 Subunit

During the course of evolution, CoVs have needed to develop a mechanism for temporarily masking the RBD until the opportunity arises to engage in receptor recognition. This masking is presumably necessary to prevent the S protein from fusing with nontarget membranes and to escape neutralization by the host humoral immune response (133). The S1 subunit of the S glycoprotein possesses an N-terminal domain (NTD) and a CTD. Both domains can engage as a receptor-binding partner of the membrane-bound host-cell receptors: SARS-CoV and MERS-CoV employ the S1 CTD (69, 75), whereas MHV utilizes its S1 NTD to bind to its receptor (126). Initial attempts to identify the RBD in a CoV resulted in the isolation of a 193-amino-acid peptide fragment (residues 318–510) of the SARS-CoV S protein that bound efficiently to ACE2 and blocked S protein–mediated infection (149). The RBD is located at the tip of the S1 subunit head and therefore lies distant from the zinc-chelating catalytic site of ACE2 when bound to the host-cell enzyme (**Figure 2**).

The crystal structure of SARS-CoV in complex with human ACE2 disclosed the fine structure of the RBD, which consists of a core and a subregion termed the RBM. This critical region contacts the complementary surface of ACE2 (67, 69). The core domain consists of five-stranded antiparallel β -sheets. The RBD possesses a subtly concave surface in the case of SARS-CoV and SARS-CoV-2 (**Figures 5** and **6**), and a flat surface in the case of MERS-CoV. The contact area of the MERS-CoV S RBD in complex with its receptor molecule, the protease DPP4, is surprisingly dominated by hydrophilic amino acid residues (75), unlike those of the SARS-CoV and SARS-CoV-2 RBDs, which include hydrophobic amino acids (see **Figure 5**).

X-ray diffraction of the CTD of SARS-CoV-2 in complex with human ACE2 at 2.5 Å resolution showed that the CTD of the S1 protein, consisting of amino acids 318–510 and containing the RBD, establishes more atomic interactions than the RBD of SARS-CoV does, an observation that correlates with biochemical data showing that SARS-CoV-2 has a higher affinity for receptor binding (143), although, as analyzed below, this is still a matter of debate. During the binding process, 20 residues in ACEs interact with 17 residues of the SARS-CoV-2 RBD (63). The area subtended at the contact interface is approximately 1,700 Å² (20, 63).

A recent molecular modeling exercise revealed the similarity between the geometric and physicochemical properties of the viral RBD–ACE2 interfaces of SARS-CoV and SARS-CoV-2 and those of antibody–antigen contacts stabilized by electrostatic interactions, suggesting that the two otherwise dissimilar systems have followed similar evolutionary maturation pathways (4).

A cryo-EM study of the full-length human ACE2 apoenzyme, alone or in complex with the RBD of the SARS-CoV-2 S protein, at 2.9-Å (3.5 Å at the RBD) resolution suggests that the RBDs of two trimers of S1 can simultaneously bind to a dimer of ACE2 molecules (159). The study was conducted in the presence of a neutral amino acid transporter, B⁰AT1, which grants stability to the crystal structure.

The affinity of the receptor for the binding partner, the S1 protein, has been assessed using a variety of approaches, with varying results. Numerical calculations derived from molecular modeling studies concluded that the SARS-CoV RBD has a higher affinity than that of SARS-CoV-2 (13); other studies indicate similar affinities (17, 146), and in some cases, SARS-CoV-2 has been demonstrated to exhibit up to 10–20 times higher affinity for ACE2 than SARS-CoV

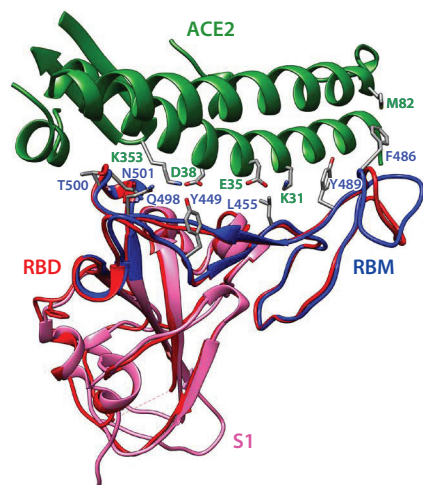


Figure 5

The S1 protein RBM–ACE2 interface. Human ACE2 (PDB ID 6M0J; *green ribbon*) is shown at the top, and the RBD of the S protein S1 subunit is shown at the bottom; the RBD of the SARS-CoV (PDB ID 2AJF) appears in red, and the SARS-CoV-2 homologous region of the S1 protein (PDB ID 6M0J) appears in magenta, with its RBM in blue. The key intervening residues at the interface are shown as sticks, labeled with the same color as the corresponding molecules. The SARS-CoV-2 RBD–ACE2 interface possesses three more salt bridges (K31, E35, and K353 from ACE2 and Q493 and G496 from the RBD) connecting the two molecules than the interface between SARS-CoV and the enzyme (63). Figure adapted from Reference 73. Distributed under a Creative Commons Attribution NonCommercial License 4.0 (CC BY-NC). Abbreviations: ACE2, angiotensin-converting enzyme 2; PDB, Protein Data Bank; RBD, receptor binding domain; RBM, receptor binding motif; S, spike; SARS-CoV, severe acute respiratory syndrome coronavirus.

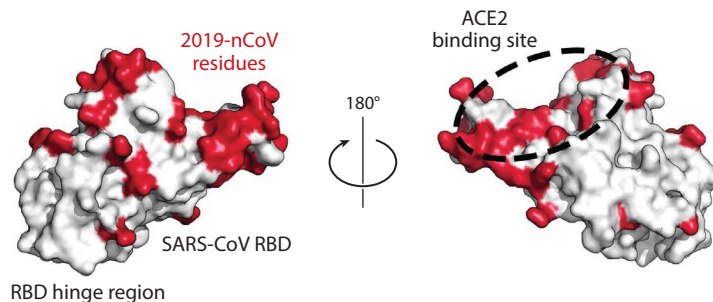


Figure 6

Comparison of the RBDs of SARS-CoV (*white*; PDB ID 2AJF) and SARS-CoV-2 (with the nomenclature of the original figure, 2019-nCoV). Residues that vary in the latter are shown in red. The binding site for landing the RBD onto ACE2 is better appreciated in the 180° rotated figure on the right (outlined with a *black dashed line*) (152). This makes the binding interface of the SARS-CoV-2 larger than that of the SARS-CoV (111). Furthermore, from the excess surface at the ridge of the SARS-CoV-2 RBD in its complex with ACE2 (63), one can infer that its RBD offers a better contact than that of SARS-CoV. These structural differences may constitute the basis of the differences in affinity of the two viruses for the common host-cell receptor, ACE2. Abbreviations: ACE2, angiotensin-converting enzyme 2; EM, electron microscopy; PDB, Protein Data Bank; RBD, receptor binding domain; SARS-CoV, severe acute respiratory virus coronavirus.

(152). Biophysical studies combining single-molecule force spectroscopy and steered molecular dynamics also support the higher strength of the interactions of SARS-CoV-2-ACE2 than the counterpart interactions of SARS-CoV with its receptor (8).

The higher affinity of SARS-CoV-2 for ACE2 is attributed to the more compact conformation of the binding ridge in its RBD and the presence of several residues in the SARS-CoV-2 RBD that stabilize two binding hot spots at the RBD-ACE2 interface (63, 111) (**Figure 6**). Lan et al. (63) found that RaTG13, a bat coronavirus closely related to SARS-CoV-2, can also use the human ACE2 as its receptor, providing new clues to the possible animal-to-human transmission of SARS-CoV-2. Similar cryo-EM work by McLellan and coworkers (152) at 3.5 Å resolution found that one of the major differences between the RBDs of the two viruses is the position in their respective down conformations, which is closer to the central cavity of the trimer in SARS-CoV-2. In the same study, the kinetics of the RBD-ACE2 interaction, quantified with surface plasmon resonance, yielded an equilibrium dissociation constant, K_d , of approximately 5 nM for the SARS-CoV-2 RBD, indicating that the ectodomain of this virus exhibits up to 10–20 times more affinity for ACE2 than does that of SARS-CoV.

Although the affinity of the RBD of SARS-CoV-2 for human ACE2 is higher than that of SARS-CoV, the affinities of the entire S proteins have been reported to be similar, or even lower, for SARS-CoV-2 (110). According to Shang et al. (110), affinities depend on the average configuration of the S protein; in SARS-CoV-2, the RBD is mostly in the down, less accessible conformer (not binding enabled), thus resulting in lower affinity. One biomedically important implication is that the hidden RBD of SARS-CoV-2 can evade immune surveillance and therefore provide insufficient immune response to COVID-19 compared to SARS.

Mainly because of its role in host-cell receptor recognition, the S1 protein subunit has dominated attention as a target for drug discovery and pharmacological intervention. Two recent preliminary molecular dynamics studies shifted the focus to the S2 subunit protein of the heterodimer (protomer of the S trimer). In the first study, two regions in the S2 subunit of the dimer and the hinge connecting the S1 and S2 subunits were identified (12). In the second study, the S2 subunit was found to exhibit much less variability and flexibility than the RBD domain in the S1 subunit (48). In addition, the latter study identified a highly conserved cavity in the SARS-CoV-2 S glycoprotein between two protomers of the trimer. The cavity can bind small macrolide-type and chitosan molecules that could destabilize the trimer, making these two small ligands potential inhibitory drugs.

When the host-cell lipid response was characterized using high-performance liquid chromatography and mass spectrometry-based lipidomics, glycerophospholipids and fatty acids were found to be significantly altered upon infection with the human coronavirus HCoV-229E; this was particularly true of the metabolism of the fatty acids linoleic acid and arachidonic acid (158). Recently, the SARS-CoV-2 S protein was produced in a secreted trimeric form using a baculovirus-Hi5 insect system. The cryo-EM structure at 2.85 Å resolution of the trimeric S protein (which occurs in the closed conformation in 70% of the cases) disclosed the presence of a tightly bound molecule of linoleic acid, an essential fatty acid, in a pocket located in each of the three RBDs (132). The hallmarks of fatty acid-binding pockets in proteins are a hydrophobic bent-tube cylindrical domain that accommodates the hydrocarbon tail and a hydrophilic domain that interacts with the acidic head-group region of the fatty acid. In the case of SARS-CoV-2, the hydrophobic domain in the RBD is mainly populated by Phe residues, and an Arg residue provides the anchor for the fatty acid head (**Figure 7**). SARS-CoV and MERS-CoV viruses harbor the same pocket, but in their case, linoleic acid stabilizes a locked conformation of the S protein that interacts less than the native conformer with its receptor *in vitro*. The linoleic acid pocket in SARS-CoV-2 may have important biomedical connotations. Linoleic acid supplementation appears to act synergistically with the drug remdesivir, suppressing SARS-CoV-2 replication in human cells *in vitro* (132).

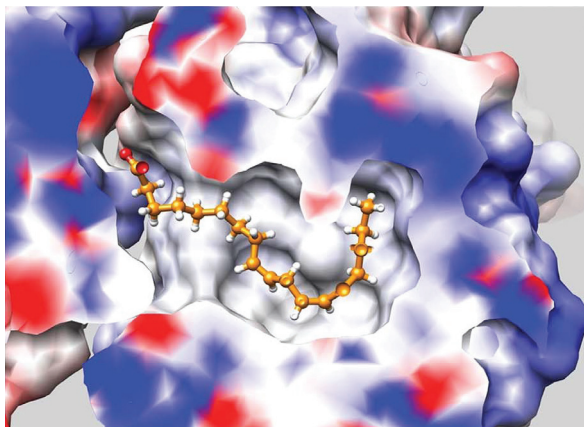


Figure 7

Surface rendering of a linoleic acid molecule (*orange stick-and-ball*) tightly bound to the SARS-CoV-2 RBD pocket. Blue and red correspond to positive and negative surface charges, respectively. Figure adapted from Reference 132, distributed under a Creative Commons Attribution Noncommercial License 4.0 (CC BY-NC). Abbreviations: RBD, receptor binding domain; SARS-CoV-2, severe acute respiratory syndrome coronavirus 2.

4. MEMBRANE FUSION: THE S2 FUSOGENIC SUBUNIT AND THE HOST-CELL PROTEASES THAT ENABLE ITS ENGAGEMENT

The intimately coupled processes of binding to and fusion with the host-cell membrane have been described as conserved mechanisms that may have followed a separate evolutionary path in different CoVs (67). According to this view, ancestral CoVs would have had a primordial spike with S2 domains only; the lack of an S1 made them functionally inefficient, relying on random diffusion across the host membrane, and membrane fusion would have thus randomly occurred in a receptor-independent manner. Gene capture would have subsequently allowed the S protein to acquire a galectin-like S1 NTD, an important evolutionary step that enhanced CoV efficiency in infecting cells. In a final evolutionary step, the S1 protein would have acquired a CTD through gene duplication of the S1 NTD (67). Comprehensive accounts of the membrane fusion mechanism can be found in recent reviews (127, 133).

Although CoVs can utilize different membrane-bound receptors and fusion mechanisms to enter cells, a generalized model of envelope membrane fusion with the host-cell plasmalemma can be considered. The model, developed during the past 15 years, involves (*a*) a molecular interaction between the virion S protein and a cell-surface enzyme acting as receptor, with or without a coreceptor; (*b*) two concerted enzymic cuts of the S glycoprotein catalyzed by two different proteases, separating S1 from the S2 subunit; and (*c*) structural rearrangements of S2 mediating the transition from the prefusion to the postfusion conformation (for a detailed review, see 133).

In the prefusion stage, three S1 receptor binding subunits of the S glycoprotein rest flat at the tip of the spike above the fusion-mediating S2 subunit, clamped down by a segment adjacent to the fusion peptide, thus preventing the S2 fusion core from undergoing the conformational transitions required for fusion (see **Figure 2**). Upon binding to ACE2, the viral S protein is cleaved by host-cell proteases at the S1–S2 interface. This constitutes the priming step, accompanied by a series of conformational transitions that enable the fusion-competent state of the S protein (88); the creation of an elongated trimeric hairpin structure formed by two heptad repeats, 1 and 2 (7); and

the release of the spike fusion peptide (the functional fusogenic element of the S protein), a process that is well characterized for SARS-CoV (56). This first step can be accomplished by several host-cell proteases, such as TMPRSS2 and cathepsins B and L, which, depending on their availability at the plasmalemma, determine viral tropism (127). TMPRSS2 is a transmembrane type 2 serine protease resident in the host-cell plasmalemma; it is hijacked by Ebola virus, CoVs, and filoviruses to infect the organism (173). TMPRSS2 is required by the three human pathogenic CoVs MERS-CoV (105, 112), SARS-CoV (82), and SARS-CoV-2 (38). When it is present, TMPRSS2 makes cells highly susceptible to SARS-CoV-2 infection (83); in fact, TMPRSS2 has been suggested to play the role of coreceptor for SARS-CoV-2 at the plasmalemma. The drug camostat blocks TMPRSS2, impeding NL63-HCoV, SARS-CoV (49), and MERS-CoV entry into cells (112). Camostat also acts as an inhibitor of Ebola virus (173). Cathepsins B and L are endosomal-resident cysteine proteases that can also produce the enzymatic dissociation of S1 and S2 in the priming step. Furthermore, furin has been demonstrated to enzymatically act at the S1/S2 site in the case of SARS-CoV-2 (152, 153).

A subsequent cleavage at a second site, S2', located upstream of the fusion peptide in S2, has been reported to activate MERS-CoV (88) but not SARS-CoV or SARS-CoV-2. Membrane fusion can occur via an early plasmalemma or via the endosomal membrane pathway, depending on the availability of the proteases at either location. SARS-CoV-2 can use both pathways (38). In the SARS-CoV-2 S protein, the redundant furin-cut motifs need to be cleaved to enable the activation (priming) of S1 and virion entry into the host cell (110). This results in the extended conformation of S2 that enables subsequent insertion of the fusion peptide into the host membrane. The free energy to overcome the energetic barrier for membrane fusion is provided by the refolding of the fusion protein from the primer prefusion conformer to the fusion-competent postfusion conformer (34). The crystal structure of the two conformers has been characterized for SARS-CoV-2 (7, 50) (**Figure 8**).

The spontaneous host-cell receptor-independent dissociation of the three S1 subunits from the S2 subunit has recently been postulated (7). This hypothesis posits that both pre- and postfusion conformations of the S protein coexist in the mature virion in a varying ratio; the extensive decoration of the S2 subunit with N-linked glycans led to the suggestion that these glycans fulfill a protective role for the postfusion conformer, should it be exposed on the surface of the mature virion, by, e.g., inducing non-neutralizing antibody responses to evade host immune reaction. EM images of naked S2 postfusion conformers on the intact virion surface seem to support this contention (25); the extended thin structures reminiscent of the postfusion S2 conformer constitute a minority of observed structures (50). Further research is required to ascertain the mechanism of virion fusion with the host-cell membranes.

5. WHAT DO THE ENDOGENOUS VIRAL PROTEASES DO?

Once the virion has penetrated the host cell, it needs to replicate its genome and produce its own proteins: structural proteins, nsps and accessory proteins. A large proportion of the CoV genome corresponds to the orfs 1a and 1ab, which are translated into the two viral replicase polyproteins pp1a and pp1ab. In both H229E-CoV (175) and SARS-CoV, these two large precursor polyproteins are in turn cleaved into 16 nsps by the chymotrypsin-like protease and the virus-encoded chymotrypsin-like 3C-like proteinase (3CL^{PRO}), also termed main protease (M^{PRO}). The nsps can thereafter engage in the production of subgenomic RNAs that encode, in turn, no less than the four structural proteins of SARS-CoV-2 (19). M^{PRO} is thus essential for the genomic and subgenomic expression and replication of the CoVs through the proteolytic processing of their replicase polyproteins.

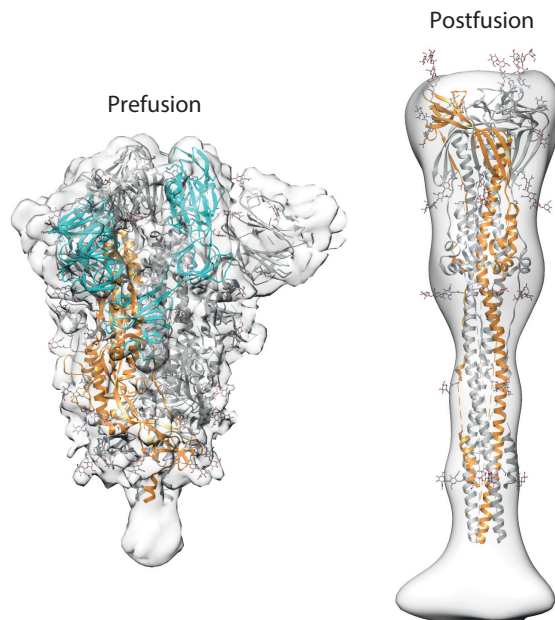


Figure 8

Prefusion and postfusion S trimer structures determined on the surface of intact SARS-CoV-2 virions by cryo-EM using subtomogram averaging. The structures are shown as transparent grey isosurfaces fitted with structures of the closed, metastable prefusion SARS-CoV-2 S trimer [PDB ID 6VXX, with one monomer colored orange (C terminus)], with its RBD in cyan (*left*) and the postfusion SARS-CoV S trimer (PDB ID 6XRA) with one subunit in orange (*right*). Image courtesy of Drs. Zulong Ke and John Briggs, Laboratory of Molecular Biology, Medical Research Council, Cambridge, UK. Abbreviations: EM, electron microscopy; PDB, Protein Data Bank; RBD, receptor binding domain; S, spike; SARS-CoV, severe acute respiratory syndrome coronavirus.

Rao and coworkers (157) determined the crystal structures of an M^{PRO} mutant from SARS-CoV and the infectious bronchitis virus. The M^{PRO} protease appears to be a challenging target for small-drug inhibition (6). The recently determined structures of SARS-CoV-2 M^{PRO} (Protein Data Bank ID 6LU7), in complex either with an α -ketoamide inhibitor (166) and two structure-based design additional inhibitors, 11a and 11b (19), or in complex with the inhibitor N3 at a resolution of 2.1 Å (47), pave the way for the development of inhibitors of the endogenous viral proteases with improved properties in comparison to current first- and second-line antiretroviral drugs in HIV therapy (114).

In SARS-CoV-2, another key endogenous viral protease is PL^{PRO}, whose atomic structure is still not known. Based on available crystallographic data of the PL^{PRO} from SARS-CoV and MERS-CoV, a recent homology modeling study found that the PL^{PRO} of SARS-CoV-2 is 97% homologous to that of a bat CoV, 80% homologous to SARS-CoV, and only 29% homologous to MERS-CoV (120).

6. STRUCTURAL KNOWLEDGE OPENS NEW AVENUES FOR DRUG, VACCINE, AND ANTIBODY DEVELOPMENTS

The structural information that has been accumulated about CoV structure has revealed potential epitopes on the virions, prompting new ideas for small drugs (see 3), vaccines (41, 72, 118, 121, 124), and neutralizing antibodies (44, 77, 154, 165) on a much more solid basis.

The differences in amino acid residues present in the RBD responsible for attachment to the cell host ACE2 (**Figure 3**) may account for the different affinities of SARS-CoV and SARS-CoV-2. As suggested by Velesler and coworkers (138), an interesting evolutionarily conserved feature of CoVs appears to be their fine-tuned balance between masking of the RBM, to limit neutralization by the humoral host immune response, and their necessary exposure, to enable receptor recognition and infection of host cells.

A wide palette of antibodies were already available against SARS-CoV and MERS-CoV; a measure of how far the field has advanced is provided by the variety of neutralizing antibodies that specifically address the RBD: monoclonal antibodies (mAbs), antigen-binding fragments (Fabs), single-chain variable region fragments (scFv), or single-domain antibodies (nanobodies) (for reviews, see 44, 174). Antibodies raised against SARS-CoV pseudovirions (i.e., an artificial construction of, e.g., a lentivirion carrying the SARS-CoV S1 protein) do not necessarily recognize epitopes in SARS-CoV-2, as is the case with T62 polyclonal antibodies (95), but other antibodies raised against pseudoviruses do cross-react with both viruses and offer therapeutic potential as neutralizing antibodies (77).

The crystal structure of the SARS-CoV S protein RBD at 2.2 Å resolution, its structure in complex with the human neutralizing antibody 80R at 2.3 Å resolution (40), and a similar structure at 2.3 Å resolution of the SARS-CoV RBD with the monoclonal antibody m396 (101) led to the conclusion that antibodies and ACE2 compete for the same highly immunogenic surfaces of the virus spike; in fact, the antibodies act as competitive inhibitor ligands of ACE2. The crystal structure of a neutralizing antibody isolated from a convalescent patient suffering from SARS, termed CR3022 (129), in complex with the RBD of the SARS-CoV-2 S protein at 3.1 Å resolution, led to the identification of a conserved epitope in the new virus, distal from the ACE2 binding site (164). Molecular modeling further suggested that the binding epitope is a cryptic site that can only be accessed by CR3022 when at least two of the three RBDs on the S protein homotrimer are in the up conformation and slightly rotated (164). The buried epitope covers an area of 917 Å², and the binding to the antibody is driven mostly by hydrophobic interactions. That this antibody generated against SARS-CoV in a SARS patient can recognize the RBD of SARS-CoV-2 can be accounted for by the high degree of amino acid conservation in the epitope (86%) (164), higher than the homology in the complete S1 protein (~77%) (171).

As this review is being written, only six months after the outbreak of the COVID-19 pandemic, new biotechnological possibilities of vaccine development have appeared. One emerging strategy is the use of viral messenger RNA (mRNA) to elicit the immune response against the spike protein. One such vaccine, known as mRNA-1273, has already gone beyond animal tests and passed phase 1 clinical trials (42); this vaccine is currently positioned at stages conventionally achieved after many more months in the making (see <https://corona.kpwwashingtonresearch.org/>). Another recent effort is the development of a preclinical SARS-CoV-2 pilot-scale vaccine candidate using as starting material strains of the virus isolated from bronchoalveolar fluid samples from 11 hospitalized patients in China and various European countries. Interestingly, the SARS-CoV-2 strains employed are widely scattered from a phylogenetic point of view. The new experimentally inactivated vaccine candidate, PiCoVacc, induced SARS-CoV-2-specific neutralizing antibodies in animal models, providing protection against a SARS-CoV-2 challenge in macaques (25). A third example is Biovacc-19, a candidate vaccine currently in the preclinical stage after passing acute toxicity testing, targeted to nonhuman-like epitopes on the SARS-CoV-2 S protein (119). Sørensen et al. (119) searched all known human proteins looking for sequence homologies with the S protein and, because the S protein exhibits 78.4% similarity with human-like epitopes, chose only nonhuman-like epitopes in their vaccine strategy to avoid autoimmune responses or antibody-induced enhancement, as observed with CoVs in animal models. A recent *in silico*

immunoinformatics approach based on immune genomics has screened regions of the S1 spike protein and the M^{PRO} protease of SARS-CoV-2 with the aim of identifying epitopes for developing vaccine candidates (96). The structural data are already providing useful hints at vaccine- and structure-guided immunogen design and raising the possibility that SARS-CoV-2 undergoes antigenic drift, as influenza viruses do (7).

The first monoclonal antibodies recently isolated from a convalescent COVID-19 patient exhibit neutralizing ability, blocking the binding of the SARS-CoV-2 S protein RBD to ACE2 (154). Another work has described the production of a human monoclonal antibody against both SARS-CoV-2 and SARS-CoV (140). The antibody, 47D11, was shown *in vitro* to bind to HEK-293T cells expressing green fluorescent protein–tagged spike proteins of the two viruses and to inhibit VeroE6 cell infection with either of the two CoVs. Wang et al. (140) suggest the possibility that the antibody destabilizes the prefusion conformation of the spike protein via receptor functional mimicry, as was previously described for the anti-SARS-CoV antibody (138). Another area of vaccine biotechnology that is acquiring momentum is structure-guided design of antigens having better immunogenic properties than those of the metastable native S protein. Along these lines, prefusion-stabilized versions of the S protein offer interesting possibilities (39). Prefusion stabilization creates immunogens that are more stable than their wild-type counterparts and increases the recombinant expression of viral fusion glycoproteins, most likely by precluding triggering or misfolding due to the protein's tendency to adopt the more stable postfusion structure. Testing combinations of substitutions led to the identification of an S protein variant with six beneficial proline substitutions that award approximately 10-fold higher expression and capacity to withstand heat stress, freeze–thaw cycles, and storage at room temperature (39). A similar approach has been followed by Briggs and coworkers (155) and Vesleer and coworkers (84), producing mutations in the S protein leading to thermostable, disulfide-bonded S-protein trimers that are trapped in the closed, prefusion state.

In summary, structural biology studies have great potential in the biotechnology of vaccine development; however, the time-constrained road ahead is not easy, and complications lie along the way, as attested to by the increasing number of immunotypes and immune responses being found in SARS-CoV-2-infected patients (81). More than 800 epitopes were recently disclosed in the SARS-CoV-2 proteome using machine learning approaches (113).

In addition to surface proteins, 16 nsps intervene in the life cycle of CoVs; some are conserved, like the RNA-dependent RNA polymerase RdRp; the main protease M^{PRO}; and nsp13, a helicase that can unwind both DNA and RNA, while others are not. A chemoproteomic analysis involving cloning, tagging, and expression of 26 out of the 29 proteins of SARS-CoV-2 in a human cell expression system disclosed an extensive, hierarchically ordered connectivity network between viral nsps and host-cell proteins, with >330 node contacts and three main hubs that disrupt the normal functions of the cell (30).

Cryo-EM and X-ray crystallography have revealed important structural–functional correlations in these diverse groups of nsps. An example is nsp3, a large multidomain protein, part of which corresponds to the enzyme ADP-ribose phosphatase or macrodomain (MacroD). This protein apparently interferes with the host immune response due to its ability to detach the ADP-ribose moiety from ADP-ribosylated proteins. The apoform of nsp3 and the complexes of the enzyme with various ligands have been solved at 1.07–2.01 Å resolution by X-ray diffraction techniques (87). Given the importance of the macrodomains in viral load, Michalska et al. (87) suggest the possible development of antiviral drugs against nsp3, pointing to the challenge of discriminating between the viral and human forms of the enzyme (24).

The nsp that is receiving the most attention is nsp12, the polymerase RdRp. The task of this protein is nothing less than to transcribe the viral genes into the adapter mRNA molecules and

replicate the approximately 32,000-nucleotide-long RNA genome. A peculiarity of viral RdRp is the error-prone character of its genome replication capacity. This apparent fault enables the viruses to rapidly undergo mutations that, e.g., improve their infectivity or adaptation to new hosts. When incorporated into a nascent RNA chain, the adenosine nucleotide analog chain terminator remdesivir acts as a broad-spectrum inhibitor of RdRp. The drug was originally developed for the treatment of the Ebola viral disease and was subsequently applied to MERS and respiratory syncytial virosis (128). Xu and coworkers (161) obtained the structure of the apoform of the SARS-CoV-2 RdRp at 2.8 Å resolution and in complex with a 50-base template-primer RNA-remdesivir at 2.5 Å resolution using cryo-EM. The study of RdRp in a conformation mimicking its active form was also tackled with cryo-EM by the Cramer group at the Max Planck Institute for Biophysical Chemistry in Göttingen (37). Detailed features of RNA processing by RdRp could be inferred from the complex of two turns of RNA, with the active site cleft of RdRp holding the first turn and two copies of nsp8 bound to opposite sides of the cleft. These two studies provide new insights into the mechanisms utilized by antivirals such as remdesivir and into the design of better inhibitors of the viral RNA polymerase. The Rao group in Shanghai studied SARS-CoV-2 RdRp in complex with the other two intervening nsps, nsp7 and nsp8, using cryo-EM at 2.9 Å resolution (26). Other very similar cryo-EM work from the same group studied the pre- and post-translocated RdRp in complex with cofactors nsp7 and nsp8, showing that the three molecules in the complex undergo significant structural rearrangements when interacting with RNA and positioning the template and primer (142). These studies facilitated *in vitro* assays of inhibitory drugs like remdesivir, leading to the conclusion that this drug causes RNA chain termination *in vitro* (29). Remdesivir has received considerable attention and has been tested against COVID-19 in clinical trials; preliminary results suggest that it may reduce the time to recovery in seriously ill patients (for a recent review, see 3). Likewise, the nsp15 endonuclease NendoU of SARS-CoV-2, which is approximately 90% homologous to that of SARS-CoV, was thought to be engaged in viral replication in a direct manner, but more recent X-ray crystallographic studies at 1.9 Å resolution suggest that it does so indirectly, by interfering with the host's immune response and thus augmenting the virulence of SARS-CoV-2 (53). Another SARS-CoV-2 nsp with high similarity to the nsps of SARS-CoV is nsp9, a protein requiring dimerization to engage in viral replication, virulence, and genomic RNA replication. An X-ray diffraction study at approximately 2 Å resolution identified a potential binding site for peptide inhibitors. At the time of writing of this article, the Protein Data Bank Europe lists more than 230 structures and 180 ligands of SARS-CoV-2 in its COVID-19 Data Portal (<https://www.ebi.ac.uk/pdbe/covid-19>).

7. ION CHANNELS IN SARS-COV-2

SARS-CoV infection requires the expression of several endogenous viral ion channel-forming proteins, also termed viroporins (74), as is also the case in other CoVs. Viroporins display an overall low degree of homology with ion channel proteins of prokaryotic or eukaryotic origin; the transmembrane regions of some of the viroporins, however, appear to have a higher degree of homology with the corresponding regions of ion channels from higher organisms, suggesting a common ancestry (23). In SARS-CoV, in between the genes coding for the S protein and the viral envelope genes there is a conserved orf region (168). One of the genes expressed in this region corresponds to orf4a, also known as the E protein, a 76–109-amino-acid protein with the capacity to form homopentameric transmembrane ion channels and regulate virus release. SARS-CoV encodes two additional ion channel proteins: orf8a and orf3a (9). Orf8a is a Cys-rich 29-amino-acid single-pass transmembrane peptide that forms cation-selective ion channels with a conductance close to 9 pS when assembled in a presumed pentameric pore in lipid bilayers (11). The

third ion channel in SARS-CoV, orf3a, has three transmembrane domains in each protomer, arranged in a homotetrameric complex *in vitro* (76), with the characteristics of a cation channel with modest selectivity for Ca^{2+} and K^{+} over Na^{+} . Suppression of orf3a expression abrogates SARS-CoV release (76), and its deletion reduces viral titer and morbidity in animal models, suggesting that orf3a-targeted drugs could find therapeutic applications in SARS and COVID-19 (51).

Given its recent discovery, our knowledge of these proteins in SARS-CoV-2 is very scant. Nuclear magnetic resonance (NMR) data of the SARS-CoV E protein transmembrane region (125) was used to map surface epitopes in the SARS-CoV-2 homologous protein (130). An NMR study showed that the E protein, when it is reconstituted in phospholipid bilayers with a composition resembling that of the ERGIC, adopts pentameric structure (80). A preliminary cryo-EM study of SARS-CoV-2 orf3a reconstituted in lipid nanodisks has recently appeared (51), showing dimers with three transmembrane segments each and tetramers structurally resembling those reported by Lu and coworkers (76) for the SARS-CoV homologous protein. The topic of ion channels in SARS-CoV-2 and other CoVs is still underdeveloped, with ample territory remaining to explore.

8. STRUCTURE–FUNCTION CORRELATIONS

Deciphering the fine structure of individual viral components is of great importance in understanding the mechanisms of pathogenic infection and for dissecting the molecular actors of the various steps (**Figure 9**). Knowledge of the virus domain(s) that binds to the cognate membrane receptor (ACE2) and engages in the recognition step is essential not only to comprehend the pathophysiology but also to design suitable strategies to inhibit these key initial steps of viral infection. The recently obtained atomic structure of the S protein trimeric complex and its two subunits S1 and S2 provided sufficient detail to delineate the interactions of this complex with its host-cell docking receptor, ACE2 (63, 110, 137, 152, 159), and calculate its affinity (17, 143, 146). Our knowledge of the ensuing enzyme-mediated conformational transitions of the S protein, which promote fusion of the virus with the host-cell plasmalemma, also benefited from recently acquired information on the enzyme cleavage sites unveiled in the structural studies (18, 110, 137). The practical implications of these structure–function correlations are readily apparent: For example, activating the expression of CD74 p41, whose canonical role is antigen presentation, was recently found to inhibit SARS-CoV-2 entry by blocking cathepsin-mediated processing and endosomal entry of the virus (5).

Once inside the cell, the viral envelope is uncoated, and the viral RNA genome is translated, initially producing the pp1a and pp1ab polypeptides. The synergistic combination of the viral proteases PL^{PRO} and M^{PRO} undertakes the proteolytic cleavage of the two polypeptides to produce nsp1, nsp2, and itself (in the case of PL^{PRO}) and the rest of the 16 mature nsps (in the case of M^{PRO}). Some of these nsps are further involved in the organization of the replication–transcription complex (RTC). The RTC is a membrane-associated RNA-protein assembly responsible for the replication of the entire RNA genome and production of subgenomic mRNAs coding for the SARS-CoV-2 structural proteins (19). Morphologically, the RTC, also called the replication organelle (RO) (115), consists of double-membrane vesicles (DMVs) approximately 250–300 nm in diameter. The most important component of the RTC is the RdRp (nsp12) (26, 37, 161), which requires the aid of nsp7 and nsp8. A recent cryo-EM tomography study of cells infected with SARS-CoV-2 revealed the existence of a pore traversing the two adjacent lipid bilayers of the DMVs, formed by six copies of nsp3, essential for viral replication (148). The viral structural proteins, together with the additional accessory orf proteins of SARS-CoV-2, are synthesized, folded—including the important trimerization of the S protein—and post-translationally modified in the ER and the ERGIC (**Figure 9**), a clear manifestation of the control exerted by the virus

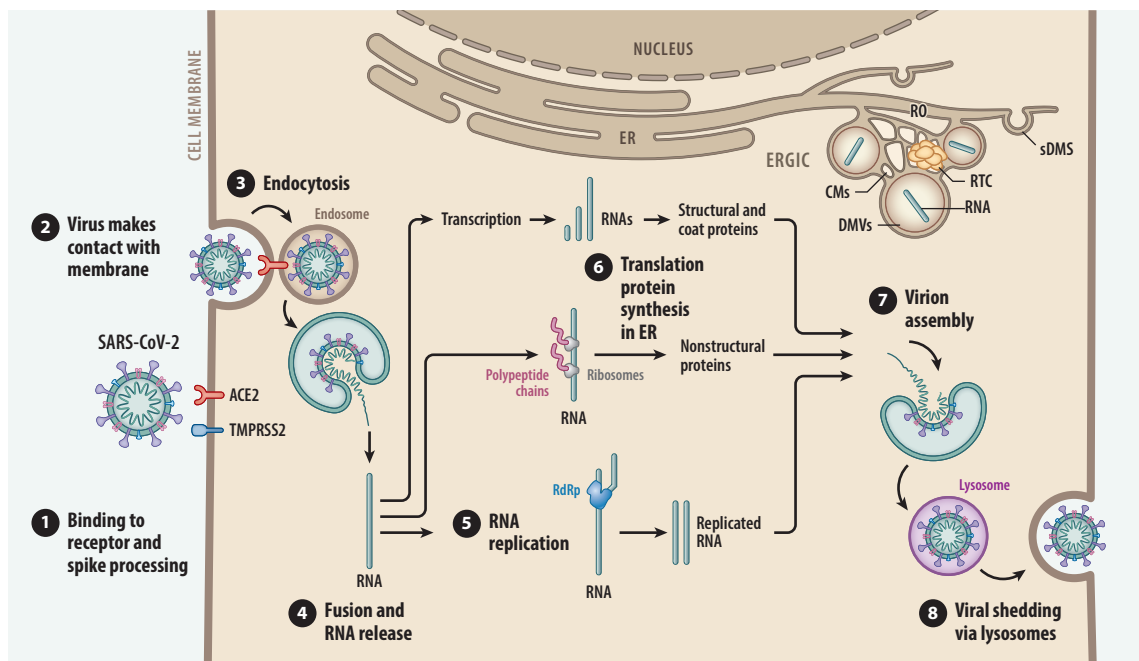


Figure 9

The life cycle of SARS-CoV-2. Shown are the different steps of the virus inside a mammalian cell, from initial binding to its cognate receptor, the membrane-bound ACE2 enzyme (step 1), to its final exit from the cell (step 8). A recent work disclosed that coronaviruses use lysosomes instead of the exocytic biosynthetic secretory pathway (27). Abbreviations: ACE2, angiotensin-converting enzyme 2; CMs, convoluted membranes; DMVs, double-membrane vesicles (a central hub for the synthesis of viral RNA); ER, endoplasmic reticulum; ERGIC, endoplasmic reticulum–Golgi intermediate compartment (where most of the post-translational modifications take place); RdRp (nsp12), RNA-dependent RNA polymerase; RO, replication organelle (the modified ERGIC subserving the replication of the viral RNA; see Reference 148); RTC, replication–transcription complex; SARS-CoV-2, severe acute respiratory syndrome coronavirus 2; sDMS, small open invaginated double-membrane spherules; TMPRSS2, transmembrane type 2 serine protease.

on the host-cell biosynthetic machinery. Additional post-translational modifications also occur in the ERGIC and the Golgi complex, where proteins initially disulfide-bonded or cotranslationally N-glycosylated at conserved sites in the ER lumen (145) are further O-glycosylated at the Golgi apparatus, thus providing another source of diversity to the repertoire of viral proteins. The orf accessory proteins adjuvate in the assembly process in the ERGIC and in the transport of the virions along the exocytic pathway.

Whereas the viral RdRp is error prone, the host-cell exocytic compartment has sophisticated control mechanisms to ensure a homeostatic balance of protein synthesis, folding, conformational stability, and degradation, generically known as proteostasis (57). The degradative arm of the proteostatic mechanism is the ER-associated degradation (ERAD) pathway, a quality-control system that avoids the clogging of the exocytic secretory pathway with excess or misfolded proteins (123). The ERAD sorts misfolded proteins to the lysosome and vacuole or to the proteasome; some proteins escape this control and are sorted at the Golgi complex. In CoV infection, ERAD-related proteins intervene in a complex termed the EDEMosome, a morphologically modified ERGIC membrane subcompartment consisting of DMVs, shared with the RTC (115). This pore enables the nascent RNA to escape the replication complex in the RO (**Figure 9**). Having completed their secretory pathway transit, mature virions are released by exocytosis, or more likely via lysosomes (27), into the extracellular medium.

9. OUTLOOK AND PROSPECTS

The mechanism of virus infection and the pathophysiology of the virus-infected cells and tissues are areas of virus research requiring further exploration and may benefit from cutting-edge biophysical approaches. Two of the hottest areas of current research efforts are undoubtedly vaccine and neutralizing antibody developments, and the S protein is a major target in both instances because of the role it plays in receptor recognition and initiation of infection. Structure-guided substitutions that increase protein yield or stability of engineered prefusion synthetic S protein (39) and engineering of human ACE2 dimers to act as a soluble decoy receptor with affinities comparable to monoclonal antibodies (10) will be two areas of intense research in the months to come. Small design decoy molecules are also potential tools to neutralize the virus. This is only part of the story: Of the new crystal structures deposited in the cryo-EM repository in 2020, roughly half correspond to proteins other than the S protein.

Organoids constitute a model system that is increasingly being applied to biomedical research. These are 3D *ex vivo* self-organized cultures derived from pluripotent stem cells, including human induced pluripotent stem cells (iPSCs) (15, 52, 85). In the specific case of SARS and COVID-19, 3D lung organoids are a step ahead of the classical 2D polarized epithelial cultures, since they can differentiate the stem cell-derived mesodermal and endodermal cells into branching airway and alveolar structures, mimicking more closely the pulmonary anatomy (100). Organoids differentiated into 3D mini-brains with several of the cytoarchitectural properties of the brain are already available (64). They have been employed to study Zika (22), SARS (100), and more recently COVID-19 (170). The latter application was recently implemented using 9-week-old brain organoids grown from iPSCs, showing the successful infection of neurons by SARS-CoV-2 and the upregulation of cell division and metabolic pathways in the infected cells (117). One can imagine exploiting the potentiality of organoids as high-throughput screening (HTS) platforms for, e.g., pharmacological small-drug, antibody, and vaccine screening. In the case of brain organoids, it is even possible to produce brain region-specific organoids using mini-bioreactors (103, 104).

Which are the most biologically relevant and urgent questions to be addressed in this area of research using structural biology and biophysical approaches? The recent advances in molecular biology of CoVs, yielding high-resolution atomic coordinates of the virus machinery's engagement with host-cell receptor molecules, has required 3D crystals for X-ray diffraction and single molecules in 2D arrangements for cryo-EM techniques. However, these powerful approaches are still incapable of interrogating an entire living cell during the infection process or observing the virus in action during its replicative cycle. Traditional transmission EM has remained the gold standard technique for conventional morphological studies of virus from a cell biology perspective, with lateral resolutions on the order of 2–5 nm and a penetration depth of approximately 500 nm (14, 167), but much like X-ray diffraction or cryo-EM, the biological specimens almost invariably need to be fixed, either chemically or physically. A mesoscale method with 3D capabilities, cryo-soft X-ray tomography of vitrified specimens, has a penetration depth of approximately 10 μm and circumvents chemical fixation (99). The technique has already been applied in cell biology in combination with single-molecule (135) or structured illumination (58) superresolution microscopies.

To delve into the realm of cell biology in action, we need to take a step back from the atomic into the nanometer scale, where we currently have the tools to image objects in live cells beyond the diffraction limit of light, i.e., the optical nanoscopies. A wide palette of techniques in optical superresolution microscopy is currently available to visualize viruses using conventional optics and visible light: the stochastic superresolution methods; the so-called single-molecule localization microscopies (SMLM), such as stochastic optical reconstruction microscopy, photoactivated

localization microscopy, or DNA points accumulation for imaging in nanoscale topography (DNA-PAINT); and the deterministic superresolution methods, such as stimulated emission depletion (STED), reversible saturable or switchable optical fluorescence transitions, or ground-state depletion microscopies, to cite the most common variants (for reviews, see 79, 108).

Minflux (2), a new form of nanoscopy, combines elements of the SMLM approach (individual on–off fluorophore switching) and the deterministic nanoscopies (an excitation beam with an intensity minimum, mimicking the doughnut in STED), affording a spatial resolution one order of magnitude better than the above classical superresolution techniques; this technique has been recently extended to the localization of molecules in 3D (32). This puts Minflux in an excellent position to study the localization of virus particles and their topographical relationship to subcellular organelles occurring at distances previously only accessible to Förster resonance energy transfer, the primary molecular ruler in fluorescence imaging to date. Ingenuity will be required to optimize the current nanoscopy instrumentation to operate under biosafety conditions adequate for handling intact, infective virions during imaging experiments with living cells. Correlative optical nanoscopy/cryo-EM offers interesting possibilities by combining mesoscale information on viral dynamics captured with superresolution optical microscopy at different stages of the replicative cycle with cryo-tomography of thin samples obtained with serial cryo-focused ion beam milling. The latter would provide fine details of the viral subcellular localization and pathogenic alterations.

By no means have biophysical methods using harsher wavelengths, such as those of electrons, been exhausted. New techniques have become available, for instance, using genetically encoded protein tags to capture gold nanoparticles, enabling visualization of individual protein molecules in a cellular environment (45). The combination of improved electron optics stability in the EM proper, cold-field emission guns optimized for narrow electron energy spread (or monochromators) to reduce chromatic aberration, next-generation direct electron detectors with improved quantum efficiency and speed, automatized data collection with subpixel accuracy, and increased computational power blended with sophisticated image processing software has produced a silent revolution in cryo-EM, making true visualization of atomic coordinates in biological macromolecules a reality. The 1.25 Å structure of the apoferritin molecule solved by the group of Holger Stark at the Max Planck Institute for Biophysical Chemistry in Göttingen, Germany (162) and the 1.7 Å resolution cryo-EM reconstruction of the β_3 GABA_A receptor, an homopentameric construct of this transmembrane ligand-gated ion channel, by Sjors Scheres' group at the Laboratory of Molecular Biology of the Medical Research Council in Cambridge in the United Kingdom (90) attest to the advances in cryo-EM resulting ultimately from a better signal-to-noise ratio (107). Progress is likely to be accomplished on other fronts, such as improvements in the preservation of biological specimens. In the specific applications covered in this review, these advances will enable the capture of different conformational states of the virus and the use of the microscope as a tool for the HTS of potential antiviral drugs.

10. CONCLUDING REMARKS

Although the first known case of HIV-1 infection occurred in 1959 in a patient in what is now the Democratic Republic of Congo, the virus was only identified, isolated, and characterized at the Pasteur Institute in Paris in 1983 and at the National Institutes of Health in Bethesda, Maryland, in 1984. SARS-CoV-2, the etiological agent of COVID-19, was identified in Wuhan, China, and its sequence posted online on January 10, 2020, only a couple of weeks after the outbreak of the “cluster of pneumonia of unknown origin,” the nosological entity that we now know as COVID-19. This acceleration attests to a very positive reaction of the scientific community in

tackling a biomedical problem of unprecedented proportions. Biophysics was probably the first scientific discipline to produce solid data in attempts to understand the etiological agent and the pathogenesis of the disease and in the search for its biomedical remediation. There are still many open paths that could contribute to these endeavors and thus help prevent future pandemics.

SUMMARY POINTS

1. Biophysics and structural biology were among the first disciplines in science to react to the new pandemic outbreak.
2. The crystal structures of the new SARS-CoV-2, alone or in complex with its host-cell receptor or other ligands, were obtained at an unprecedented pace, partly thanks to the structural biology groundwork in the preceding two decades.
3. The novel findings have shone new light on important mechanistic aspects of viral infection. Probably the best-studied facet is the recognition of the viral S proteins by host-cell surface receptors.
4. In the case of SARS-CoV-2, the etiological agent of COVID-19, new information about the atomic structure of its S glycoprotein bound to the membrane-bound metalloprotease ACE2 has greatly advanced our understanding of the initial step in the infective process.
5. New structurally and functionally important motifs have been disclosed in both structural and nonstructural proteins of the new virus.
6. Key mechanistic information conducive to the development of structure-based inhibitory design drugs, neutralizing antibodies, and vaccines has been produced within a few weeks.
7. As a direct result, various prophylactic and therapeutic tools are being developed at an unparalleled pace.

FUTURE ISSUES

1. Structural research addressed at unraveling structure–function correlations will continue to help us gain a better understanding of the still unresolved and biomedically important mechanisms operating in viral infection.
2. The recent developments in single-particle cryo-EM, having achieved visualization of individual atoms in intact proteins, will facilitate the identification of specific sites and motifs in the viral structure amenable to inhibition by design drugs.
3. Likewise, the most recent developments in optical microscopy (nanoscopy) may open new avenues to explore the virus cycle in living cells.
4. The combined use of structural and electrophysiological biophysical techniques may prove useful in tackling the study of viral ion channel proteins (viroporins) in SARS-CoV-2 for interventional purposes.
5. Structure-based design approaches will increasingly be applied to the development and production of more stable immunogenic SARS-CoV-2 fragments and decoy molecules to neutralize the virus.

DISCLOSURE STATEMENT

The author is not aware of any affiliations, memberships, funding, or financial holdings that might be perceived as affecting the objectivity of this review.

ACKNOWLEDGMENTS

This work was written within the framework of grants PICT 2015–2654 from the Ministry of Science, Technology and Innovative Production of Argentina and PIP 853 from the Scientific and Technological Research Council of Argentina (CONICET). I would like to apologize to all authors whose work I have not been able to include in this review. Due to the unprecedented pace of discovery in the field, important new results are appearing as I write these lines. I am grateful to Dr. Mariano Dellarole for valuable discussions.

LITERATURE CITED

1. Almeida JD, Tyrrell DA. 1967. The morphology of three previously uncharacterized human respiratory viruses that grow in organ culture. *J. Gen. Virol.* 1:175–78
2. Balzarotti F, Eilers Y, Gwosch KC, Gynnå AH, Westphal V, et al. 2017. Nanometer resolution imaging and tracking of fluorescent molecules with minimal photon fluxes. *Science* 355:606–12
3. Barrantes FJ. 2020. While we wait for a vaccine against SARS-CoV-2, why not think about available drugs? *Front. Physiol.* 11:820
4. Brielle ES, Schneidman-Duhovny D, Linial M. 2020. The SARS-CoV-2 exerts a distinctive strategy for interacting with the ACE2 human receptor. *Viruses* 12:497
5. Bruchez A, Sha K, Johnson J, Chen L, Stefani C, et al. 2020. MHC class II transactivator CIITA induces cell resistance to Ebola virus and SARS-like coronaviruses. *Science* 970:241–47
6. Bzówka M, Mitusińska K, Raczyńska A, Samol A, Tuszyński JA, Góra A. 2020. Structural and evolutionary analysis indicate that the SARS-CoV-2 Mpro is a challenging target for small-molecule inhibitor design. *Int. J. Mol. Sci.* 21:3099
7. Cai Y, Zhang J, Xiao T, Peng H, Sterling SM, et al. 2020. Distinct conformational states of SARS-CoV-2 spike protein. *Science* 369:1586–92
8. Cao W, Dong C, Kim S, Hou D, Tai W, et al. 2020. Biomechanical characterization of SARS-CoV-2 spike RBD and human ACE2 protein-protein interaction. *bioRxiv* 230730. <https://doi.org/10.1101/2020.07.31.230730>
9. Castaño-Rodríguez C, Honrubia JM, Gutiérrez-Álvarez J, DeDiego ML, Nieto-Torres JL, et al. 2018. Role of severe acute respiratory syndrome coronavirus viroporins E, 3a, and 8a in replication and pathogenesis. *mBio* 9:e02325–17
10. Chan KK, Dorosky D, Sharma P, Abbasi SA, Dye JM, et al. 2020. Engineering human ACE2 to optimize binding to the spike protein of SARS coronavirus 2. *Science* 369:1261–65
11. Chen C-C, Krüger J, Sramala I, Hsu H-J, Henklein P, et al. 2011. ORF8a of SARS-CoV forms an ion channel: experiments and molecular dynamics simulations. *Biochim. Biophys. Acta Biomembr.* 1808:572–79
12. Chen SH, Young MT, Gounley J, Stanley C, Bhowmik D. 2020. Distinct structural flexibility within SARS-CoV-2 spike protein reveals potential therapeutic targets. *bioRxiv* 047548. <https://doi.org/10.1101/2020.04.17.047548>
13. Chen Y, Guo Y, Pan Y, Zhao ZJ. 2020. Structure analysis of the receptor binding of 2019-nCoV. *Biochem. Biophys. Res. Commun.* 525:135–40
14. Chong MK, Chua AJ, Tan TT, Tan SH, Ng ML. 2014. Microscopy techniques in flavivirus research. *Micron* 59:33–43
15. Clevers H. 2016. Modeling development and disease with organoids. *Cell* 165:1586–97
16. Colebatch HJ, Ng CK. 1992. Estimating alveolar surface area during life. *Respir. Physiol.* 88:163–70
17. Corrêa Giron C, Laaksonen A, Barroso da Silva FL. 2020. On the interactions of the receptor-binding domain of SARS-CoV-1 and SARS-CoV-2 spike proteins with monoclonal antibodies and the receptor ACE2. *Virus Res.* 285:198021

18. Coutard B, Valle C, de Lamballerie X, Canard B, Seidah NG, Decroly E. 2020. The spike glycoprotein of the new coronavirus 2019-nCoV contains a furin-like cleavage site absent in CoV of the same clade. *Antivir. Res.* 176:104742
19. Dai W, Zhang B, Su H, Li J, Zhao Y, et al. 2020. Structure-based design of antiviral drug candidates targeting the SARS-CoV-2 main protease. *Science* 368:1331–35
20. De Sancho D, Perez-Jimenez R, Gavira JA. 2020. Coarse-grained molecular simulations of the binding of the SARS-CoV 2 spike protein RBD to the ACE2 cell receptor. bioRxiv 083212. <https://doi.org/10.1101/2020.05.07.083212>
21. Díaz J. 2020. SARS-CoV-2 molecular network structure. *Front. Physiol.* 11:870
22. Fischer S. 2017. Minibrain storm: Cerebral organoids aren't real brains? But they provide a powerful platform for modeling brain diseases like Zika infection, Alzheimer's, and even autism. *IEEE Pulse* 8:31–34
23. Fischer WB, Hsu H-J. 2011. Viral channel forming proteins—modeling the target. *Biochim. Biophys. Acta Biomembr.* 1808:561–71
24. Frick DN, Viridi RS, Vuksanovic N, Dahal N, Silvaggi NR. 2020. Molecular basis for ADP-ribose binding to the Mac1 domain of SARS-CoV-2 nsp3. *Biochemistry* 59:2608–15
25. Gao Q, Bao L, Mao H, Wang L, Xu K, et al. 2020. Rapid development of an inactivated vaccine candidate for SARS-CoV-2. *Science* 369:77–81
26. Gao Y, Yan L, Huang Y, Liu F, Zhao Y, et al. 2020. Structure of the RNA-dependent RNA polymerase from COVID-19 virus. *Science* 368:779–82
27. Ghosh S, Dellibovi-Ragheb TA, Kerviel A, Pak E, Qui Q, et al. 2020. B-Coronaviruses use lysosomes for egress instead of the biosynthetic secretory pathway. *Cell* 183:1520–35
28. Gonzalez JM, Gomez-Puertas P, Cavanagh D, Gorbalenya AE, Enjuanes L. 2003. A comparative sequence analysis to revise the current taxonomy of the family Coronaviridae. *Arch. Virol.* 148:2207–35
29. Gordon CJ, Tchesnokov EP, Woolner E, Perry JK, Feng JY, et al. 2020. Remdesivir is a direct-acting antiviral that inhibits RNA-dependent RNA polymerase from severe acute respiratory syndrome coronavirus 2 with high potency. *J. Biol. Chem.* 295:6785–97
30. Gordon DE, Jang GM, Bouhaddou M, Xu J, Obernier K, et al. 2020. A SARS-CoV-2 protein interaction map reveals targets for drug repurposing. *Nature* 583:459–68
31. Guan WJ, Ni ZY, Hu Y, Liang WH, Ou CQ, et al. 2020. Clinical characteristics of coronavirus disease 2019 in China. *N. Engl. J. Med.* 382:1708–20
32. Gwosch KC, Pape JK, Balzarotti F, Hoess P, Ellenberg J, et al. 2020. MINFLUX nanoscopy delivers 3D multicolor nanometer resolution in cells. *Nat. Methods* 17:217–24
33. Hamming I, Timens W, Bulthuis ML, Lely AT, Navis G, van Goor H. 2004. Tissue distribution of ACE2 protein, the functional receptor for SARS coronavirus: a first step in understanding SARS pathogenesis. *J. Pathol.* 203:631–37
34. Harrison SC. 2015. Viral membrane fusion. *Virology* 479–80:498–507
35. Helander HF, Fändriks L. 2014. Surface area of the digestive tract—revisited. *Scand. J. Gastroenterol.* 49:681–89
36. Hikmet F, Méar L, Edvinsson Å, Micke P, Uhlén M, Lindskog C. 2020. The protein expression profile of ACE2 in human tissues. *Mol. Syst. Biol.* 16:e9610
37. Hillen HS, Kokic G, Farnung L, Dienemann C, Tegunov D, Cramer P. 2020. Structure of replicating SARS-CoV-2 polymerase. *Nature* 584:154–56
38. Hoffmann M, Kleine-Weber H, Schroeder S, Krüger N, Herrler T, et al. 2020. SARS-CoV-2 cell entry depends on ACE2 and TMPRSS2 and is blocked by a clinically proven protease inhibitor. *Cell* 181:271–80.e8
39. Hsieh C-L, Goldsmith JA, Schaub JM, DiVenere AM, Kuo H-C, et al. 2020. Structure-based design of prefusion-stabilized SARS-CoV-2 spikes. *Science* 369:1501–5
40. Hwang WC, Lin Y, Santelli E, Sui J, Jaroszewski L, et al. 2006. Structural basis of neutralization by a human anti-severe acute respiratory syndrome spike protein antibody, 80R. *J. Biol. Chem.* 281:34610–16
41. Imai Y, Kuba K, Rao S, Huan Y, Guo F, et al. 2005. Angiotensin-converting enzyme 2 protects from severe acute lung failure. *Nature* 436:112–16

42. Jackson LA, Anderson EJ, Roupael NG, Roberts PC, Makhene M, et al. 2020. An mRNA vaccine against SARS-CoV-2—preliminary report. *N. Engl. J. Med.* 383:1920–31
43. Jia HP, Look DC, Shi L, Hickey M, Pewe L, et al. 2005. ACE2 receptor expression and severe acute respiratory syndrome coronavirus infection depend on differentiation of human airway epithelia. *J. Virol.* 79:14614–21
44. Jiang S, Hillyer C, Du L. 2020. Neutralizing antibodies against SARS-CoV-2 and other human coronaviruses. *Trends Immunol.* 41:355–59
45. Jiang Z, Jin X, Li Y, Liu S, Liu X-M, et al. 2020. Genetically encoded tags for direct synthesis of EM-visible gold nanoparticles in cells. *Nat. Methods* 17:937–46
46. Jin X, Lian JS, Hu JH, Gao J, Zheng L, et al. 2020. Epidemiological, clinical and virological characteristics of 74 cases of coronavirus-infected disease 2019 (COVID-19) with gastrointestinal symptoms. *Gut* 69:1002–9
47. Jin Z, Du X, Xu Y, Deng Y, Liu M, et al. 2020. Structure of M(pro) from SARS-CoV-2 and discovery of its inhibitors. *Nature* 582:289–93
48. Kalathiya U, Padariya M, Mayordomo M, Lisowska M, Nicholson J, et al. 2020. Highly conserved homotrimer cavity formed by the SARS-CoV-2 spike glycoprotein: a novel binding site. *J. Clin. Med.* 9:1473
49. Kawase M, Shirato K, van der Hoek L, Taguchi F, Matsuyama S. 2012. Simultaneous treatment of human bronchial epithelial cells with serine and cysteine protease inhibitors prevents severe acute respiratory syndrome coronavirus entry. *J. Virol.* 86:6537–45
50. Ke Z, Oton J, Qu K, Cortese M, Zila V, et al. 2020. Structures and distributions of SARS-CoV-2 spike proteins on intact virions. *Nature* 588:498–502
51. Kern DM, Sorum B, Hoel CM, Sridharan S, Remis JP, et al. 2020. Cryo-EM structure of the SARS-CoV-2 3a ion channel in lipid nanodiscs. bioRxiv 156554. <https://doi.org/10.1101/2020.06.17.156554>
52. Kim J, Koo B-K, Knoblich JA. 2020. Human organoids: model systems for human biology and medicine. *Nat. Rev. Mol. Cell Biol.* 21:571–84
53. Kim Y, Jedrzejczak R, Maltseva NI, Wilamowski M, Endres M, et al. 2020. Crystal structure of Nsp15 endoribonuclease NendoU from SARS-CoV-2. *Protein Sci.* 29:1596–605
54. Kimura H, Francisco D, Conway M, Martinez FD, Vercelli D, et al. 2020. Type 2 inflammation modulates ACE2 and TMPRSS2 in airway epithelial cells. *J. Allergy Clin. Immunol.* 146:80–88.e8
55. Kirchdoerfer RN, Cottrell CA, Wang N, Pallesen J, Yassine HM, et al. 2016. Pre-fusion structure of a human coronavirus spike protein. *Nature* 531:118–21
56. Kirchdoerfer RN, Wang N, Pallesen J, Wrapp D, Turner HL, et al. 2018. Stabilized coronavirus spikes are resistant to conformational changes induced by receptor recognition or proteolysis. *Sci. Rep.* 8:15701
57. Klaips CL, Jayaraj GG, Hartl FU. 2018. Pathways of cellular proteostasis in aging and disease. *J. Cell Biol.* 217:51–63
58. Kounatidis I, Stanifer ML, Phillips MA, Paul-Gilloteaux P, Heiligenstein X, et al. 2020. 3D correlative cryo-structured illumination fluorescence and soft X-ray microscopy elucidates reovirus intracellular release pathway. *Cell* 182:515–30.e17
59. Krijnse-Locker J, Ericsson M, Rottier PJ, Griffiths G. 1994. Characterization of the budding compartment of mouse hepatitis virus: evidence that transport from the RER to the Golgi complex requires only one vesicular transport step. *J. Cell Biol.* 124:55–70
60. Kubo H, Yamada YK, Taguchi F. 1994. Localization of neutralizing epitopes and the receptor-binding site within the amino-terminal 330 amino acids of the murine coronavirus spike protein. *J. Virol.* 68:5403–10
61. Lai MM, Cavanagh D. 1997. The molecular biology of coronaviruses. *Adv. Virus Res.* 48:1–100
62. Lamers MM, Beumer J, van der Vaart J, Knoops K, Puschhof J, et al. 2020. SARS-CoV-2 productively infects human gut enterocytes. *Science* 369:50–54
63. Lan J, Ge J, Yu J, Shan S, Zhou H, et al. 2020. Structure of the SARS-CoV-2 spike receptor-binding domain bound to the ACE2 receptor. *Nature* 581:215–20
64. Lee CT, Bendriem RM, Wu WW, Shen RF. 2017. 3D brain organoids derived from pluripotent stem cells: promising experimental models for brain development and neurodegenerative disorders. *J. Biomed. Sci.* 24:59

65. Letko M, Miazgowicz K, McMinn R, Seifert SN, Sola I, et al. 2018. Adaptive evolution of MERS-CoV to species variation in DPP4. *Cell Rep.* 24:1730–37
66. Li F. 2013. Receptor recognition and cross-species infections of SARS coronavirus. *Antiv. Res.* 100:246–54
67. Li F. 2016. Structure, function, and evolution of coronavirus spike proteins. *Annu. Rev. Virol.* 3:237–61
68. Li F, Berardi M, Li W, Farzan M, Dormitzer PR, Harrison SC. 2006. Conformational states of the severe acute respiratory syndrome coronavirus spike protein ectodomain. *J. Virol.* 80:6794–800
69. Li F, Li W, Farzan M, Harrison SC. 2005. Structure of SARS coronavirus spike receptor-binding domain complexed with receptor. *Science* 309:1864–68
70. Li W, Hulswit RJG, Kenney SP, Widjaja I, Jung K, et al. 2018. Broad receptor engagement of an emerging global coronavirus may potentiate its diverse cross-species transmissibility. 115:E5135–43
71. Li W, Hulswit RJG, Widjaja I, Raj VS, McBride R, et al. 2017. Identification of sialic acid-binding function for the Middle East respiratory syndrome coronavirus spike glycoprotein. *PNAS* 114:E8508–17
72. Li W, Moore MJ, Vasilieva N, Sui J, Wong SK, et al. 2003. Angiotensin-converting enzyme 2 is a functional receptor for the SARS coronavirus. *Nature* 426:450–54
73. Li X, Giorgi EE, Marichannegowda MH, Foley B, Xiao C, et al. 2020. Emergence of SARS-CoV-2 through recombination and strong purifying selection. *Sci. Adv.* 6:eabb9153
74. Liao Y, Tam JP, Liu DX. 2006. Viroporin activity of SARS-CoV E protein. *Adv. Exp. Med. Biol.* 581:199–202
75. Lu G, Hu Y, Wang Q, Qi J, Gao F, et al. 2013. Molecular basis of binding between novel human coronavirus MERS-CoV and its receptor CD26. *Nature* 500:227–31
76. Lu W, Zheng BJ, Xu K, Schwarz W, Du L, et al. 2006. Severe acute respiratory syndrome-associated coronavirus 3a protein forms an ion channel and modulates virus release. *PNAS* 103:12540–45
77. Lv Z, Deng Y-Q, Ye Q, Cao L, Sun C-Y, et al. 2020. Structural basis for neutralization of SARS-CoV-2 and SARS-CoV by a potent therapeutic antibody. *Science* 369:1505–9
78. Macneughton MR, Davies HA. 1978. Ribonucleoprotein-like structures from coronavirus particles. *J. Gen. Virol.* 39:545–49
79. Mahecic D, Testa I, Griffie J, Manley S. 2019. Strategies for increasing the throughput of super-resolution microscopies. *Curr. Opin. Chem. Biol.* 51:84–91
80. Mandala VS, McKay MJ, Shcherbakov AA, Dregni AJ, Kolokouris A, Hong M. 2020. Structure and drug binding of the SARS-CoV-2 envelope protein in phospholipid bilayers. *Nat. Struct. Mol. Biol.* 27:1202–8
81. Mathew D, Giles JR, Baxter AE, Oldridge DA, Greenplate AR, et al. 2020. Deep immune profiling of COVID-19 patients reveals distinct immunotypes with therapeutic implications. *Science* 369:eabc8511
82. Matsuyama S, Nagata N, Shirato K, Kawase M, Takeda M, Taguchi F. 2010. Efficient activation of the severe acute respiratory syndrome coronavirus spike protein by the transmembrane protease TMPRSS2. *J. Virol.* 84:12658–64
83. Matsuyama S, Nao N, Shirato K, Kawase M, Saito S, et al. 2020. Enhanced isolation of SARS-CoV-2 by TMPRSS2-expressing cells. *PNAS* 117:7001–3
84. McCallum M, Walls A, Bowen JE, Corti D, Veesler D. 2020. Structure-guided covalent stabilization of coronavirus spike glycoprotein trimers in the closed conformation. *Nat. Struct. Mol. Biol.* 27:942–49
85. McCauley HA, Wells JM. 2017. Pluripotent stem cell-derived organoids: using principles of developmental biology to grow human tissues in a dish. *Development* 144:958–62
86. Mehdipour AR, Hummer G. 2020. Dual nature of human ACE2 glycosylation in binding to SARS-CoV-2 spike. bioRxiv 193680. <https://doi.org/10.1101/2020.07.09.193680>
87. Michalska K, Kim Y, Jedrzejczak R, Maltseva NI, Stols L, et al. 2020. Crystal structures of SARS-CoV-2 ADP-ribose phosphatase: from the apo form to ligand complexes. *IUCr* 7:814–24
88. Millet JK, Whittaker GR. 2015. Host cell proteases: critical determinants of coronavirus tropism and pathogenesis. *Virus Res.* 202:120–34
89. Mortola E, Roy P. 2004. Efficient assembly and release of SARS coronavirus-like particles by a heterologous expression system. *FEBS Lett.* 576:174–78
90. Nakane T, Kotecha A, Sente A, McMullan G, Masiulis S, et al. 2020. Single-particle cryo-EM at atomic resolution. *Nature* 587:152–56

91. Natesh R, Schwager SLU, Sturrock ED, Acharya KR. 2003. Crystal structure of the human angiotensin-converting enzyme-lisinopril complex. *Nature* 421:551–54
92. Neuman BW, Adair BD, Yoshioka C, Quispe JD, Orca G, et al. 2006. Supramolecular architecture of severe acute respiratory syndrome coronavirus revealed by electron cryomicroscopy. *J. Virol.* 80:7918–28
93. Neuman BW, Buchmeier MJ. 2016. Supramolecular architecture of the coronavirus particle. *Adv. Virus Res.* 96:1–27
94. Neuman BW, Kiss G, Kunding AH, Bhella D, Baksh MF, et al. 2011. A structural analysis of M protein in coronavirus assembly and morphology. *J. Struct. Biol.* 174:11–22
95. Ou X, Liu Y, Lei X, Li P, Mi D, et al. 2020. Characterization of spike glycoprotein of SARS-CoV-2 on virus entry and its immune cross-reactivity with SARS-CoV. *Nat. Commun.* 11:1620
96. Panda PK, Arul MN, Patel P, Verma SK, Luo W, et al. 2020. Structure-based drug designing and immunoinformatics approach for SARS-CoV-2. *Sci. Adv.* 6:eabb8097
97. Park YJ, Walls AC, Wang Z, Sauer MM, Li W, et al. 2019. Structures of MERS-CoV spike glycoprotein in complex with sialoside attachment receptors. *Nat. Struct. Mol. Biol.* 26:1151–57
98. Patel AB, Verma A. 2020. Nasal ACE2 levels and COVID-19 in children. *JAMA* 323:2386–87
99. Pereiro E. 2019. Correlative cryo-soft X-ray tomography of cells. *Biophys. Rev.* 11:529–30
100. Porotto M, Ferren M, Chen YW, Siu Y, Makhous N, et al. 2019. Authentic modeling of human respiratory virus infection in human pluripotent stem cell-derived lung organoids. *mbio* 10(3):e00723-19
101. Prabakaran P, Gan J, Feng Y, Zhu Z, Choudhry V, et al. 2006. Structure of severe acute respiratory syndrome coronavirus receptor-binding domain complexed with neutralizing antibody. *J. Biol. Chem.* 281:15829–36
102. Prabakaran P, Xiao X, Dimitrov DS. 2004. A model of the ACE2 structure and function as a SARS-CoV receptor. *Biochem. Biophys. Res. Commun.* 314:235–41
103. Qian X, Jacob F, Song MM, Nguyen HN, Song H, Ming GL. 2018. Generation of human brain region-specific organoids using a miniaturized spinning bioreactor. *Nat. Protoc.* 13:565–80
104. Qian X, Nguyen HN, Song MM, Hadiono C, Ogden SC, et al. 2016. Brain-region-specific organoids using mini-bioreactors for modeling ZIKV exposure. *Cell* 165:1238–54
105. Qian Z, Dominguez SR, Holmes KV. 2013. Role of the spike glycoprotein of human Middle East respiratory syndrome coronavirus (MERS-CoV) in virus entry and syncytia formation. *PLOS ONE* 8:e76469
106. Richardson S, Hirsch JS, Narasimhan M, Crawford JM, McGinn T, et al. 2020. Presenting characteristics, comorbidities, and outcomes among 5700 patients hospitalized with COVID-19 in the New York City area. *JAMA* 323:2052–59
107. Rosenthal PB, Henderson R. 2003. Optimal determination of particle orientation, absolute hand, and contrast loss in single-particle electron cryomicroscopy. *J. Mol. Biol.* 333:721–45
108. Sahl SJ, Hell SW, Jakobs S. 2017. Fluorescence nanoscopy in cell biology. *Nat. Rev. Mol. Cell Biol.* 18:685–701
109. Scheller C, Krebs F, Minkner R, Astner I, Gil-Moles M, Wätzig H. 2020. Physicochemical properties of SARS-CoV-2 for drug targeting, virus inactivation and attenuation, vaccine formulation and quality control. *Electrophoresis* 41:1137–51
110. Shang J, Wan Y, Luo C, Ye G, Geng Q, et al. 2020. Cell entry mechanisms of SARS-CoV-2. *PNAS* 117:11727–34
111. Shang J, Ye G, Shi K, Wan Y, Luo C, et al. 2020. Structural basis of receptor recognition by SARS-CoV-2. *Nature* 581:221–24
112. Shirato K, Kawase M, Matsuyama S. 2013. Middle East respiratory syndrome coronavirus infection mediated by the transmembrane serine protease TMPRSS2. *J. Virol.* 87:12552–61
113. Shrock E, Fujimura E, Kula T, Timms RT, Lee I-H, et al. 2020. Viral epitope profiling of COVID-19 patients reveals cross-reactivity and correlates of severity. *Science* 370(6520):eabd4250
114. Sisay M. 2020. 3CL(pro) inhibitors as a potential therapeutic option for COVID-19: available evidence and ongoing clinical trials. *Pharmacol. Res.* 156:104779
115. Snijder EJ, Limpens R, de Wilde AH, de Jong AWM, Zevenhoven-Dobbe JC, et al. 2020. A unifying structural and functional model of the coronavirus replication organelle: tracking down RNA synthesis. *PLOS Biol.* 18:e3000715

116. Sok D, Pauthner M, Briney B, Lee JH, Saye-Francisco KL, et al. 2016. A prominent site of antibody vulnerability on HIV envelope incorporates a motif associated with CCR5 binding and its camouflaging glycans. *Immunity* 45:31–45
117. Song E, Zhang C, Israelow B, Lu P, Weizman O-E, et al. 2020. Neuroinvasive potential of SARS-CoV-2 revealed in a human brain organoid model. *bioRxiv* 169946. <https://doi.org/10.1101/2020.06.25.169946>
118. Song W, Gui M, Wang X, Xiang Y. 2018. Cryo-EM structure of the SARS coronavirus spike glycoprotein in complex with its host cell receptor ACE2. *PLOS Pathog.* 14:e1007236
119. Sørensen B, Susrud A, Dalglish AG. 2020. Biovacc-19: a candidate vaccine for Covid-19 (SARS-CoV-2) developed from analysis of its general method of action for infectivity. *QRB Discov.* 1:e6
120. Stoermer M. 2020. Homology models of the papain-like protease PLpro from coronavirus 2019-nCoV. *chemRxiv*. https://chemrxiv.org/articles/Homology_Models_of_the_Papain-Like_Protease_PLpro_from_Coronavirus_2019-nCoV/11799705
121. Struck A-W, Axmann M, Pfefferle S, Drosten C, Meyer B. 2012. A hexapeptide of the receptor-binding domain of SARS corona virus spike protein blocks viral entry into host cells via the human receptor ACE2. *Antivir. Res.* 94:288–96
122. Su S, Wong G, Shi W, Liu J, Lai ACK, et al. 2016. Epidemiology, genetic recombination, and pathogenesis of coronaviruses. *Trends Microbiol.* 24:490–502
123. Sun Z, Brodsky JL. 2019. Protein quality control in the secretory pathway. *J. Cell Biol.* 218:3171–87
124. Supekar VM, Bruckmann C, Ingallinella P, Bianchi E, Pessi A, Carfi A. 2004. Structure of a proteolytically resistant core from the severe acute respiratory syndrome coronavirus S2 fusion protein. *PNAS* 101:17958–63
125. Surya W, Li Y, Torres J. 2018. Structural model of the SARS coronavirus E channel in LMPG micelles. *Biochim. Biophys. Acta Biomembr.* 1860:1309–17
126. Taguchi F, Hirai-Yuki A. 2012. Mouse hepatitis virus receptor as a determinant of the mouse susceptibility to MHV infection. *Front. Microbiol.* 3:68
127. Tang T, Bidon M, Jaimes JA, Whittaker GR, Daniel S. 2020. Coronavirus membrane fusion mechanism offers a potential target for antiviral development. *Antivir. Res.* 178:104792
128. Tchesnokov EP, Feng JY, Porter DP, Götte M. 2019. Mechanism of inhibition of Ebola virus RNA-dependent RNA polymerase by remdesivir. *Viruses* 11:326
129. ter Meulen J, van den Brink EN, Poon LL, Marissen WE, Leung CS, et al. 2006. Human monoclonal antibody combination against SARS coronavirus: synergy and coverage of escape mutants. *PLOS Med.* 3:e237
130. Tilocca B, Soggiu A, Sanguinetti M, Babini G, De Maio F, et al. 2020. Immunoinformatic analysis of the SARS-CoV-2 envelope protein as a strategy to assess cross-protection against COVID-19. *Microbes Infect.* 22:182–87
131. To J, Surya W, Torres J. 2016. Targeting the channel activity of viroporins. *Adv. Protein Chem. Struct. Biol.* 104:307–55
132. Toelzer C, Gupta K, Yadav SKN, Borucu U, Davidson AD, et al. 2020. Free fatty acid binding pocket in the locked structure of SARS-CoV-2 spike protein. *Science* 370:725–30
133. Tortorici MA, Veesler D. 2019. Structural insights into coronavirus entry. *Adv. Virus Res.* 105:93–116
134. Towler P, Staker B, Prasad SG, Menon S, Tang J, et al. 2004. ACE2 X-ray structures reveal a large hinge-bending motion important for inhibitor binding and catalysis. *J. Biol. Chem.* 279:17996–8007
135. Varsano N, Dadosh T, Kapishnikov S, Pereiro E, Shimoni E, et al. 2016. Development of correlative cryo-soft X-ray tomography and stochastic reconstruction microscopy: a study of cholesterol crystal early formation in cells. *J. Am. Chem. Soc.* 138:14931–40
136. Venkatagopalan P, Daskalova SM, Lopez LA, Dolezal KA, Hogue BG. 2015. Coronavirus envelope (E) protein remains at the site of assembly. *Virology* 478:75–85
137. Walls AC, Park YJ, Tortorici MA, Wall A, McGuire AT, Veesler D. 2020. Structure, function, and antigenicity of the SARS-CoV-2 spike glycoprotein. *Cell* 181:281–92
138. Walls AC, Xiong X, Park YJ, Tortorici MA, Snijder J, et al. 2019. Unexpected receptor functional mimicry elucidates activation of coronavirus fusion. *Cell* 176:1026–39.e15

139. Wan Y, Shang J, Graham R, Baric RS, Li F. 2020. Receptor recognition by the novel coronavirus from Wuhan: an analysis based on decade-long structural studies of SARS coronavirus. *J. Virol.* 94:e00127-20
140. Wang C, Li W, Drabek D, Okba NMA, van Haperen R, et al. 2020. A human monoclonal antibody blocking SARS-CoV-2 infection. *Nat. Commun.* 11:2251
141. Wang K, Chen W, Zhou Y-S, Lian J-Q, Zhang Z, et al. 2020. SARS-CoV-2 invades host cells via a novel route: CD147-spike protein. *Signal Transduct. Target. Ther.* 5:283
142. Wang Q, Wu J, Wang H, Gao Y, Liu Q, et al. 2020. Structural basis for RNA replication by the SARS-CoV-2 polymerase. *Cell* 182:417–28.e13
143. Wang Q, Zhang Y, Wu L, Niu S, Song C, et al. 2020. Structural and functional basis of SARS-CoV-2 entry by using human ACE2. *Cell* 181:894–904.e9
144. Deleted in proof
145. Watanabe Y, Allen JD, Wrapp D, McLellan JS, Crispin M. 2020. Site-specific glycan analysis of the SARS-CoV-2 spike. *Science* 369:330–33
146. Wells SA. 2020. Rigidity, normal modes and flexible motion of a SARS-CoV-2 (COVID-19) protease structure. bioRxiv 986190. <https://doi.org/10.1101/2020.03.10.986190>
147. Wiener RS, Cao YX, Hinds A, Ramirez MI, Williams MC. 2007. Angiotensin converting enzyme 2 is primarily epithelial and is developmentally regulated in the mouse lung. *J. Cell Biochem.* 101:1278–91
148. Wolff G, Limpens RWAL, Zevenhoven-Dobbe JC, Laugks U, Zheng S, et al. 2020. A molecular pore spans the double membrane of the coronavirus replication organelle. *Science* 369:1395–98
149. Wong SK, Li W, Moore MJ, Choe H, Farzan M. 2004. A 193-amino acid fragment of the SARS coronavirus S protein efficiently binds angiotensin-converting enzyme 2. *J. Biol. Chem.* 279:3197–201
150. Woo PCY, Lau SKP, Lam CSF, Tsang AKL, Hui S-W, et al. 2014. Discovery of a novel bottlenose dolphin coronavirus reveals a distinct species of marine mammal coronavirus in gammacoronavirus. *J. Virol.* 88:1318–31
151. Wrapp D, McLellan JS. 2020. The 3.1-Angstrom cryo-electron microscopy structure of the porcine epidemic diarrhea virus spike protein in the prefusion conformation. *J. Virol.* 93:e00923-19
152. Wrapp D, Wang N, Corbett KS, Goldsmith JA, Hsieh CL, et al. 2020. Cryo-EM structure of the 2019-nCoV spike in the prefusion conformation. *Science* 367:1260–63
153. Wu K, Li W, Peng G, Li F. 2009. Crystal structure of NL63 respiratory coronavirus receptor-binding domain complexed with its human receptor. *PNAS* 106:19970–74
154. Wu Y, Wang F, Shen C, Peng W, Li D, et al. 2020. A noncompeting pair of human neutralizing antibodies block COVID-19 virus binding to its receptor ACE2. *Science* 368:1274–78
155. Xiong X, Qu K, Ciazynska KA, Hosmillo M, Carter AP, et al. 2020. A thermostable, closed SARS-CoV-2 spike protein trimer. *Nat. Struct. Mol. Biol.* 27:934–41
156. Xu H, Zhong L, Deng J, Peng J, Dan H, et al. 2020. High expression of ACE2 receptor of 2019-nCoV on the epithelial cells of oral mucosa. *Int. J. Oral Sci.* 12:8
157. Xue X, Yu H, Yang H, Xue F, Wu Z, et al. 2008. Structures of two coronavirus main proteases: implications for substrate binding and antiviral drug design. *J. Virol.* 82:2515–27
158. Yan B, Chu H, Yang D, Sze KH, Lai PM, et al. 2019. Characterization of the lipidomic profile of human coronavirus-infected cells: implications for lipid metabolism remodeling upon coronavirus replication. *Viruses* 11:73
159. Yan R, Zhang Y, Li Y, Xia L, Guo Y, Zhou Q. 2020. Structural basis for the recognition of SARS-CoV-2 by full-length human ACE2. *Science* 367:1444–48
160. Ye Y, Hogue BG. 2007. Role of the coronavirus E viroporin protein transmembrane domain in virus assembly. *J. Virol.* 81:3597–607
161. Yin W, Mao C, Luan X, Shen D-D, Shen Q, et al. 2020. Structural basis for inhibition of the RNA-dependent RNA polymerase from SARS-CoV-2 by remdesivir. *Science* 368:1499–504
162. Yip KM, Fischer N, Paknia E, Chari A, Stark H. 2020. Atomic resolution protein structure determination by cryo-EM. *Nature* 587(7832):157–61
163. Yu J, Qiao S, Guo R, Wang X. 2020. Cryo-EM structures of HKU2 and SARS-CoV spike glycoproteins provide insights into coronavirus evolution. *Nat. Commun.* 11:3070
164. Yuan M, Wu NC, Zhu X, Lee CD, So RTY, et al. 2020. A highly conserved cryptic epitope in the receptor binding domains of SARS-CoV-2 and SARS-CoV. *Science* 368:630–33

165. Yuan Y, Cao D, Zhang Y, Ma J, Qi J, et al. 2017. Cryo-EM structures of MERS-CoV and SARS-CoV spike glycoproteins reveal the dynamic receptor binding domains. *Nat. Commun.* 8:15092
166. Zhang L, Lin D, Sun X, Curth U, Drosten C, et al. 2020. Crystal structure of SARS-CoV-2 main protease provides a basis for design of improved α -ketoamide inhibitors. *Science* 368:409–12
167. Zhang P. 2019. Advances in cryo-electron tomography and subtomogram averaging and classification. *Curr. Opin. Struct. Biol.* 58:249–58
168. Zhang R, Wang K, Lv W, Yu W, Xie S, et al. 2014. The ORF4a protein of human coronavirus 229E functions as a viroporin that regulates viral production. *Biochim. Biophys. Acta Biomembr.* 1838:1088–95
169. Zhang Y, Kutaleladze TG. 2020. Molecular structure analyses suggest strategies to therapeutically target SARS-CoV-2. *Nat. Commun.* 11:2920
170. Zhou H, Liu LP, Fang M, Li YM, Zheng YW. 2020. A potential ex vivo infection model of human induced pluripotent stem cell-3D organoids beyond coronavirus disease 2019. *Histol. Histopathol.* 35(10):1077–82
171. Zhou P, Yang X-L, Wang X-G, Hu B, Zhang L, et al. 2020. A pneumonia outbreak associated with a new coronavirus of probable bat origin. *Nature* 579:270–73
172. Zhou T, Tsybovsky Y, Gorman J, Rapp M, Cerutti G, et al. 2020. Cryo-EM structures of SARS-CoV-2 spike without and with ACE2 reveal a pH-dependent switch to mediate endosomal positioning of receptor-binding domains. *Cell Host Microbe* 28:867–79.e5
173. Zhou Y, Vedantham P, Lu K, Agudelo J, Carrion R Jr., et al. 2015. Protease inhibitors targeting coronavirus and filovirus entry. *Antivir. Res.* 116:76–84
174. Zhou Y, Yang Y, Huang J, Jiang S, Du L. 2019. Advances in MERS-CoV vaccines and therapeutics based on the receptor-binding domain. *Viruses* 11:60
175. Ziebuhr J, Siddell SG. 1999. Processing of the human coronavirus 229E replicase polypeptides by the virus-encoded 3C-like proteinase: identification of proteolytic products and cleavage sites common to pp1a and pp1ab. *J. Virol.* 73:177–85
176. Ziegler CGK, Allon SJ, Nyquist SK, Mbano IM, Miao VN, et al. 2020. SARS-CoV-2 receptor ACE2 is an interferon-stimulated gene in human airway epithelial cells and is detected in specific cell subsets across tissues. *Cell* 181:1016–35.e19



Contents

Review of COVID-19 Antibody Therapies <i>Jiabui Chen, Kaifu Gao, Rui Wang, Duc Duy Nguyen, and Guo-Wei Wei</i>	1
The Mechanosensory Transduction Machinery in Inner Ear Hair Cells <i>Wang Zheng and Jeffrey R. Holt</i>	31
Structure of Phycobilisomes <i>Sen-Fang Sui</i>	53
Biophysics of Chromatin Remodeling <i>Ilana M. Nodelman and Gregory D. Bowman</i>	73
Structures and Functions of Chromatin Fibers <i>Ping Chen, Wei Li, and Guohong Li</i>	95
From Bench to Keyboard and Back Again: A Brief History of Lambda Phage Modeling <i>Michael G. Cortes, Yiruo Lin, Lanying Zeng, and Gábor Balázs</i>	117
Recent Developments in the Field of Intrinsically Disordered Proteins: Intrinsic Disorder–Based Emergence in Cellular Biology in Light of the Physiological and Pathological Liquid–Liquid Phase Transitions <i>Vladimir N. Uversky</i>	135
Biophysics of Notch Signaling <i>David Sprinzak and Stephen C. Blacklow</i>	157
Bayesian Inference: The Comprehensive Approach to Analyzing Single-Molecule Experiments <i>Colin D. Kinz-Thompson, Korak Kumar Ray, and Ruben L. Gonzalez Jr.</i>	191
Learning to Model G-Quadruplexes: Current Methods and Perspectives <i>Iker Ortiz de Luzuriaga, Xabier Lopez, and Adrià Gil</i>	209
Analysis of Tandem Repeat Protein Folding Using Nearest-Neighbor Models <i>Mark Petersen and Doug Barrick</i>	245

Biomolecular Modeling and Simulation: A Prospering Multidisciplinary Field <i>Tamar Schlick, Stephanie Portillo-Ledesma, Christopher G. Myers, Lauren Beljak, Justin Chen, Sami Dakbel, Daniel Darling, Sayak Ghosh, Joseph Hall, Mikael Jan, Emily Liang, Sera Saju, Mackenzie Vohr, Chris Wu, Yifan Xu, and Eva Xue</i>	267
Biomolecular Systems Engineering: Unlocking the Potential of Engineered Allostery via the Lactose Repressor Topology <i>Thomas M. Groseclose, Ronald E. Rondon, Ashley N. Hersey, Prasaad T. Milner, Dowan Kim, Fumin Zhang, Matthew J. Reaflff, and Corey J. Wilson</i>	303
Directed Evolution of Microbial Communities <i>Álvaro Sánchez, Jean C.C. Vila, Chang-Yu Chang, Juan Diaz-Colunga, Sylvie Estrela, and María Rebolleda-Gomez</i>	323
The Molecular Basis for Life in Extreme Environments <i>Nozomi Ando, Blanca Barquera, Douglas H. Bartlett, Eric Boyd, Audrey A. Burnim, Amanda S. Byer, Daniel Colman, Richard E. Gillilan, Martin Gruebele, George Makhatadze, Catherine A. Royer, Everett Shock, A. Joshua Wand, and Maxwell B. Watkins</i>	343
The Sliding Filament Theory Since Andrew Huxley: Multiscale and Multidisciplinary Muscle Research <i>Joseph D. Powers, Sage A. Malingen, Michael Regnier, and Thomas L. Daniel</i>	373
How Physical Interactions Shape Bacterial Biofilms <i>Berenike Maier</i>	401
Cutting-Edge Single-Molecule Technologies Unveil New Mechanics in Cellular Biochemistry <i>Souradeep Banerjee, Soham Chakraborty, Abhijit Sreepada, Devshuvam Banerji, Shashwat Goyal, Yajushi Khurana, and Shubbasis Haldar</i>	419
Measuring Absolute Membrane Potential Across Space and Time <i>Julia R. Lazzari-Dean, Anneliese M.M. Gest, and Evan W. Miller</i>	447
Advancing Biophysics Using DNA Origami <i>Wouter Engelen and Hendrik Dietz</i>	469
The Contribution of Biophysics and Structural Biology to Current Advances in COVID-19 <i>Francisco J. Barrantes</i>	493
Protein Reconstitution Inside Giant Unilamellar Vesicles <i>Thomas Litschel and Petra Schwille</i>	525
Structure and Mechanics of Dynein Motors <i>John T. Canty, Ruensern Tan, Emre Kusakci, Jonathan Fernandes, and Ahmet Yildiz</i>	549

The Phasor Plot: A Universal Circle to Advance Fluorescence Lifetime Analysis and Interpretation <i>Leonel Malacrida, Suman Ranjit, David M. Jameson, and Enrico Gratton</i>	575
Molecular Force Measurement with Tension Sensors <i>Lisa S. Fischer, Srishti Rangarajan, Tanmay Sadhanasatish, and Carsten Grashoff</i>	595

Indexes

Cumulative Index of Contributing Authors, Volumes 46–50	617
---	-----

Errata

An online log of corrections to *Annual Review of Biophysics articles* may be found at
<http://www.annualreviews.org/errata/biophys>